AD-A131 360 AERODYNAMICS OF ADVANCED AXIAL-FLOW TURBOMACHINERY(U) 1/1
IOWA STATE UNIV AMES ENGINEERING RESEARCH INST
G K SEROVY ET AL. FEB 83 ISU-ERI-AMES-83234
UNCLASSIFIED AFOSR-TR-83-0651 AFOSR-81-0004 F/G 21/5 NL

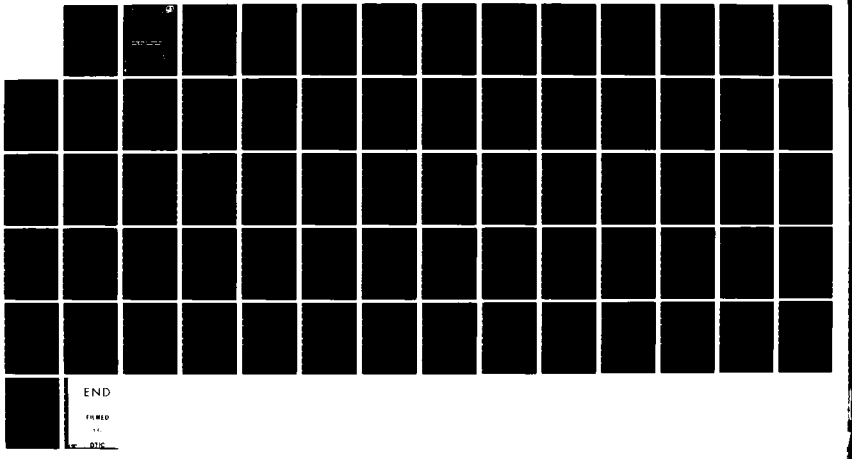

END

FILMED

DTIC

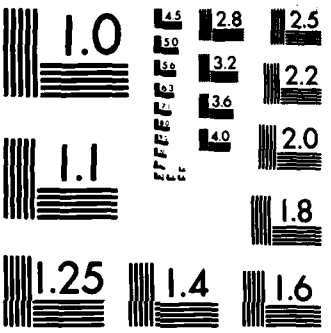

George K. Serovy
Patrick Kavanagh
Theodore H. Okiishi

February 1983

Aerodynamics of Advanced Axial-Flow Turbomachinery

Final Report: 1 October 1980—30 November 1982

TURBOMACHINERY
RESEARCH PROGRAM

Approved for Public Release; Distribution Unlimited

ENGINEERING RESEARCH INSTITUTE
IOWA STATE UNIVERSITY
AMES, IOWA 50010 USA

ENGINEERING RESEARCH
ENGINEERING RESEARCH
ENGINEERING RESEARCH
ENGINEERING RESEARCH
ENGINEERING RESEARCH

Aerodynamics of Advanced Axial-Flow Turbomachinery

Final Report

1 October 1980–30 November 1982

George K. Serovy
Patrick Kavanagh
Theodore H. Okiishi

February 1983

ISU-ERI-Ames-83234
TCRL-23
Projects 1489-1491

Turbomachinery Components Research Laboratory
Department of Mechanical Engineering
Engineering Research Institute
Iowa State University; Ames, Iowa 50011

UNCLASSIFIED

SECURITY CLASSIFICATION OF THIS PAGE (When Data Entered) iii

REPORT DOCUMENTATION PAGE	READ INSTRUCTIONS BEFORE COMPLETING FORM
1. REPORT NUMBER **AFOSR-TR- 83-0651** 2. GOVT ACCESSION NO. AD-A131360	3. RECIPIENT'S CATALOG NUMBER
4. TITLE (and Subtitle) AERODYNAMICS OF ADVANCED AXIAL-FLOW TURBOMACHINERY	5. TYPE OF REPORT & PERIOD COVERED Report: Final 1 Oct. 1980-30 Nov. 1982
	6. PERFORMING ORG. REPORT NUMBER TCRL-23
7. AUTHOR(s) George K. Serovy Patrick Kavanagh T. H. Okiishi	8. CONTRACT OR GRANT NUMBER(s) AFOSR-81-0004
9. PERFORMING ORGANIZATION NAME AND ADDRESS Engineering Research Institute Iowa State University Ames, Iowa 50011	10. PROGRAM ELEMENT, PROJECT, TASK AREA & WORK UNIT NUMBERS 61102F 2307/A4
11. CONTROLLING OFFICE NAME AND ADDRESS Air Force Office of Scientific Research Directorate of Aerospace Sciences (AFOSR/NA) Bldg. 410, Bolling Air Force Base, Washington,DC	12. REPORT DATE February 1983 13. NUMBER OF PAGES 72
14. MONITORING AGENCY NAME & ADDRESS(if different from Controlling Office)	15. SECURITY CLASS. (of this report) Unclassified 15a. DECLASSIFICATION/DOWNGRADING SCHEDULE

16. DISTRIBUTION STATEMENT (of this Report)

Approved for Public Release; Distribution Unlimited

17. DISTRIBUTION STATEMENT (of the abstract entered in Block 20, if different from Report)

18. SUPPLEMENTARY NOTES

19. KEY WORDS (Continue on reverse side if necessary and identify by block number)

axial-flow turbomachinery
axial-flow compressor
axial-flow turbine
cascade aerodynamics
computational fluid mechanics
turbomachine flow measurement

20. ABSTRACT (Continue on reverse side if necessary and identify by block number)

A multi-task research program on the aerodynamics of advanced axial-flow turbomachinery was completed at Iowa State University. Program components were intended to result in direct contributions to the improvement of axial-flow fan, compressor, and turbine design procedures. A detailed experimental investigation of intrapassage flow in a large-scale, curved, rectangular cross-section channel representative of turbomachinery passages was carried out. The use of stator geometry modification to improve stage performance through

DD FORM 1 JAN 73 1473 EDITION OF 1 NOV 65 IS OBSOLETE

UNCLASSIFIED

SECURITY CLASSIFICATION OF THIS PAGE (When Data Entered)

better secondary flow control was investigated via laboratory tests of baseline and modified versions of a two-stage compressor. Aerodynamic variables which influence surface boundary layer development in compressor and turbine airfoil cascades were restudied in order to determine sources of differences between linear cascade performance and performance of equivalent cascade geometries in multistage turbomachine blade rows. Parameters associated with steady flow as well as those connected with blade-passing frequency (wake generated) unsteady entrance region flow were considered. This final report volume summarizes the progress achieved during the grant period. Details are contained in separate volumes of the final report series.

TABLE OF CONTENTS

LIST OF FIGURES

LIST OF TABLES

SECTION I. INTRODUCTION

The Turbomachinery Components Research Program at Iowa State University is involved in experimental and analytical fluid mechanics research projects covering a wide range of turbomachinery applications. These projects have been supported for some twenty-five years by government agencies, including the National Aeronautics and Space Administration (NASA), the United States Air Force Office of Scientific Research (USAF/AFOSR), the United States Air Force Aero Propulsion Laboratory (USAF/AFAPL), the Naval Air Systems Command, the National Science Foundation (NSF), and various industrial concerns. A research project involving aerodynamic studies of advanced axial-flow turbomachinery, as discussed in this summary report and other volumes of the final report series, was initiated in October 1978 under funding through AFOSR Contract F49620-79-C-0002. Highlights of the results of three individual tasks, namely, an analysis of secondary flow and associated losses in blade passages, an assessment of modifications of stator blade row geometries to control end-wall flows in compressors for improved performance, and an evaluation of the influence of blade surface boundary layer and wake prediction models based on comparisons of experimental cascade and rotating blade row data are discussed in the following section.

SECTION II. RESULTS OF THE RESEARCH PROGRAM

Highlights of the results of each of the three tasks in the research program are discussed in this section. Task I originated as internally-supported work at Iowa State University and is based on earlier analyses carried out with support from the Pratt and Whitney Group of the United Technologies Corporation. The results provide further knowledge of the complex, three-dimensional internal flows involved in curved channels, and they have been used to assess the usefulness of computer codes which were intended to model similar flow situations. Task II evolved from discussions with Dr. Arthur J. Wennerstrom of AFAPL and has resulted in fundamental design data that will be usable in future high efficiency multistage axial-flow compressor development. Task III is based on problems in modernization of compressor design systems developed previously during research on deviation angle prediction sponsored by the Air Force (AFAPL, AFOSR), NASA and AGARD. The results of this task suggest additions to blade performance correlations and improvments in boundary-layer computation systems.

TASK I: EXPERIMENTAL AND ANALYTICAL INVESTIGATION OF FLOW IN A CURVED RECTANGULAR CROSS-SECTION PASSAGE

Introduction

In the design of high performance gas turbine engines, it is essential to be able to account properly for the effects of three-dimensional flows occurring within blade passages of the turbine and compressor. The objective of work summarized here has been to provide insight into the mechanism of three-dimensional and secondary flows in a curved passage, and to investigate quantitatively the relationship between the inlet endwall boundary layer characteristics and the generated secondary losses. The results obtained are based on experimental measurements made in air for a large-scale, 90-deg. curved rectangular cross-section passage representative of a turbine cascade passage. Five-hole, Kiel and hot-film probe measurements were obtained at the inlet section to the passage and in cross sections in the curved and straight discharge portions of the passage to map out the three-dimensional detail of the passage mean flow. A total of twelve cross sections (measurement traverse planes) in the curved portion and discharge section of the passage were involved. Complete documentation of the test rig, experimental procedures, data reduction and compilations, and analysis of results is contained in References 1-4.

Cascade losses are generally dealt with in terms of (1) profile losses resulting from boundary layer growth over the blade surfaces and (2) secondary losses caused by the endwall boundary layers and their three-dimensional interaction with the primary flow over the

blade surfaces. These latter losses, the main subject of the present investigation, are termed "secondary" since they relate to the transverse flow velocity components in the blade passages. Secondary losses may, in fact, account for over half the total losses incurred; they become increasingly important and dominant as the blade aspect ratio for the cascade decreases.

As an outcome of turning of the flow through the cascade, cross-passage pressure gradients are established which promote the development of endwall flow towards the blade suction surface. Ahead of the cascade, the inlet boundary layer separates from the endwall to form a horseshoe vortex, with one leg of the vortex extending into one blade passage and the other into the adjacent passage. The first leg moves across the endwall toward the suction surface corner, merging with the strong crossflow in the newly formed endwall boundary layer within the cascade to form a passage vortex. The other leg of the horseshoe vortex continues along the suction surface corner as a counter vortex. In total, the crossflow produced sweeps low momentum fluid of the inlet endwall boundary layer toward the blade suction surface where, through roll-up of the passage vortex toward midspan and interaction with the suction surface boundary layer, a line of flow separation is produced along the suction surface.

Three-dimensional and secondary flow studies carried out in the past for cascades can be placed in one of two categories, based on the particular objectives of the work. The first of these categories involves the calculation of transverse flow velocities from the normal component of vorticity. The second involves relating measured losses

to empirically formulated loss correlation coefficients. In this latter case the majority of blade passage and conventional cascade testing has measured only exit plane total pressure and primary flow velocities with the goal of evaluating turning angle and pressure loss coefficient. Detailed intrapassage measurements are required, however, to thoroughly understand cascade losses and the contributing development of endwall flows and secondary losses. Flow visualization of the passage vortex by Herzig and Hansen [5,6] was among the earliest efforts to investigate three-dimensional flow in cascades. Armstrong [7] carried out turbine cascade tests to investigate the effect of inlet boundary layer thickness on losses. Moore and Richards [8] measured the intrapassage streamwise and pitchwise velocity components in a compressor cascade. Turner [9], measuring the pressure and flow velocities in the inlet and outlet planes of a cascade of high-turning nozzles, and Senoo [10], using the same cascade for intrapassage measurements with a thin laminar and a natural turbulent inlet boundary layer, concluded that similar streamwise velocity profile patterns existed. Different transverse flow velocity profiles were observed, however, and were concluded to be functions of the inlet vorticity. Senoo also observed endwall boundary layer accumulation and roll-up onto the suction surface.

The studies noted above have been useful in providing information on total pressure and velocity distributions in cascades. However, more complete information is needed to describe the secondary loss nature and loss generation, some of which has been provided by more recent testing. Belik [11,12] investigated the nature and distribution

of secondary losses in a linear cascade of low aspect ratio and high turning. From profile and endwall skin friction loss measurements, Belik concluded that secondary loss was the principal result of intense flow separation in the suction corner, and that the corner separation loss could be proportional to the mass flow into the corner. Came [13] conducted a detailed study of the inlet boundary layer thickness effect on secondary loss in linear cascades. He concluded that secondary losses increase with increasing displacement thickness up to 5 percent of chord; beyond this point the losses remained constant.

A detailed study of the complete three-dimensional flow field inside a large-scale linear turbine cascade was conducted by Langston et al. [14]. This study clearly detected all major characteristics of secondary flow (i.e., endwall crossflow, boundary layer roll-up, vortex formation, etc.). Large total pressure losses were measured, which were caused by extensive vortex interaction with the primary flow. Langston [15] in examining his test results further has determined an analytical model for the endwall crossflow away from regions of three-dimensional separation.

Flow tests complementary to cascade testing have also been made on curved channels. Joy [16] measured total pressures in ducts having 90 and 180 deg. of turning, and evaluated the direction of the secondary flow from the distortion of the Bernoulli surfaces. Further details of the secondary flow in curved, rectangular ducts were obtained by Eichenberger [17]. Bruun [18] carried out detailed total pressure measurements in two large-scale curved rectangular passages of 120 deg.

turning. He found the kinetic energy of the secondary flow to be less than 10 percent of the total losses and concluded, therefore, that the major part of the secondary losses resulted from laminar and turbulent dissipation within the passage. Most recently, McMillan [19] reported the results of tests on a low-speed turbulent flow in a diffusing bend with the objective of providing detailed mean flow data suitable for comparison with calculation.

Summary of Test Passage Results

The flow field within the test passage was determined from probe measurements in the traverse planes and from static-tap pressure measurements on the sidewalls and endwalls. In addition, flow visualizations of the limiting streamlines on the passage walls were obtained.

Four different test cases (identified as Cases C, D, E and F) based on the inlet endwall boundary layer were involved. The boundary layer velocity profiles for the four cases were essentially two-dimensional, extending from endwall-to-endwall symmetrically about midspan. The four test cases, which provided a range of momentum thickness for the inlet endwall boundary layer, were used to investigate the effects of endwall boundary layer characteristics on the passage secondary flows and losses. Table I summarizes these characteristics along with relevant flow information for the test cases.

Table I. Summary of inlet endwall boundary layer characteristics, Reynolds number, average q_o and traverse plane measurements made. H is the passage span.

Test Case	Boundary Layer Thickness/H	Displacement Thickness θ*inlet/H	Momentum Thickness θ*inlet/H	Reynolds Number[1]	Average Freestream q_o in H_2O	Traverse Plane Probe Used	Traverse Planes Measured
C	0.2570	0.0211	0.0174	1.05×10^6	3.57	5-hole	3,4,5,8,9, 10,11,12
D	0.0569	0.0052	0.0045	1.32×10^6	5.67	5-hole	1-12
E	0.0944	0.0101	0.0079	1.11×10^6	4.00	Kiel	3,4,5,6,7, 9,11,12
F	0.3131	0.0258	0.0220	0.96×10^6	2.95	Kiel	3,4,5,6,7, 9,12

[1]Based on inlet conditions and inlet plane hydraulic diameter.

Total Pressure Losses

The mass-averaged total pressure loss coefficient, $\bar{C}pt$, for the measured traverse planes in the test cases is shown in Figure 1, where Cpt is defined as the change in total pressure from the inlet ratioed to the inlet dynamic pressure, q_o. This coefficient is obtained by carrying out a mass-weighted integration of the local total pressure coefficient, Cpt, over the traverse planes or cross sections of the passage. The coefficients $\bar{C}pt$ constitute passage losses plus the momentum defect in the inlet velocity profile, and truly represent a loss coefficient. Flow angle data obtained from five-hole probe measurements were used in obtaining the mass-weighted integrations.

The different behavior of the loss coefficient through the passage is noted in Figure 1 for the four test cases. In Test Case F ($\theta^*_{inlet}/H = 0.022$) $\bar{C}pt$ is appreciably greater throughout the passage than for the other three cases, with values continuing to increase at a uniform rate to the end of the passage. By contrast, in Test Case D ($\theta^*_{inlet}/H = 0.0045$) and Test Case E ($\theta^*_{inlet}/H = 0.0079$), it is observed that $\bar{C}pt$ increases rapidly in the middle portion of the passage and then tends to level off to some lower value than for Test Case F. The loss curve for Test Case C ($\theta^*_{inlet}/H = 0.0175$) agrees more with that for Test Case F except that the loss level is lower, corresponding to the lower inlet endwall boundary layer momentum thickness. In each of the cases, the size and loss levels of the passage vortex at any given point in the passage tend to

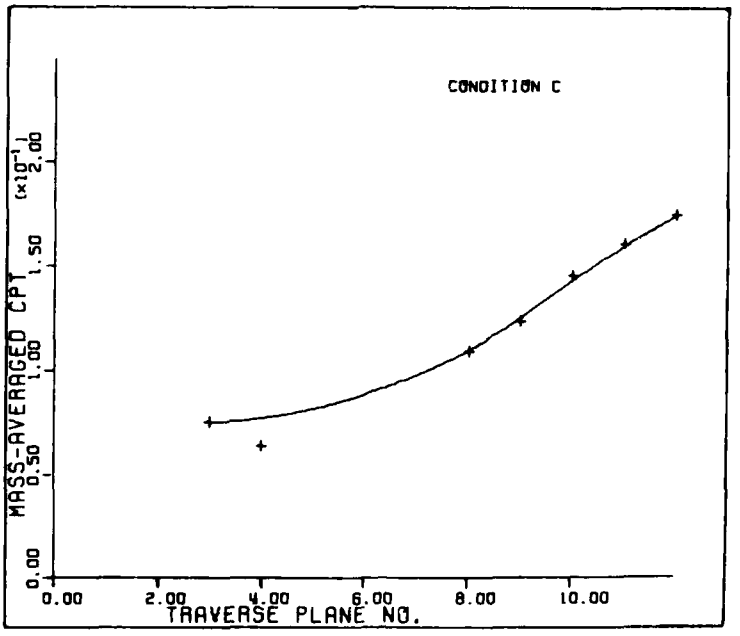

TEST CASE C

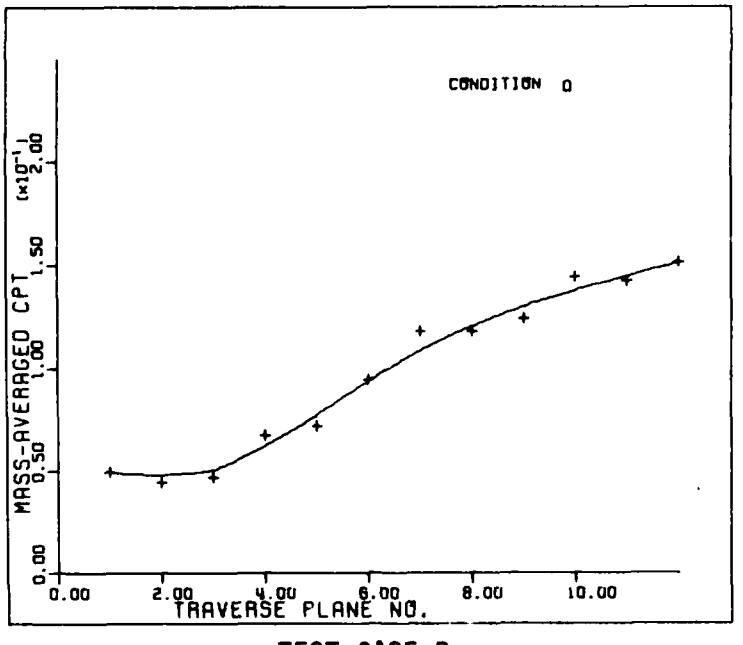

TEST CASE D

Figure 1. Mass-averaged total pressure loss coefficient vs. traverse plane for the four test cases.

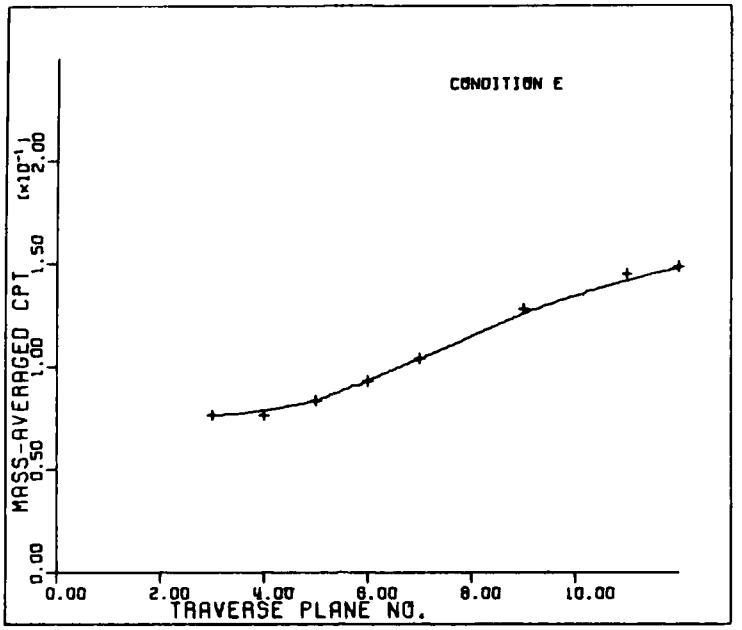

TEST CASE E

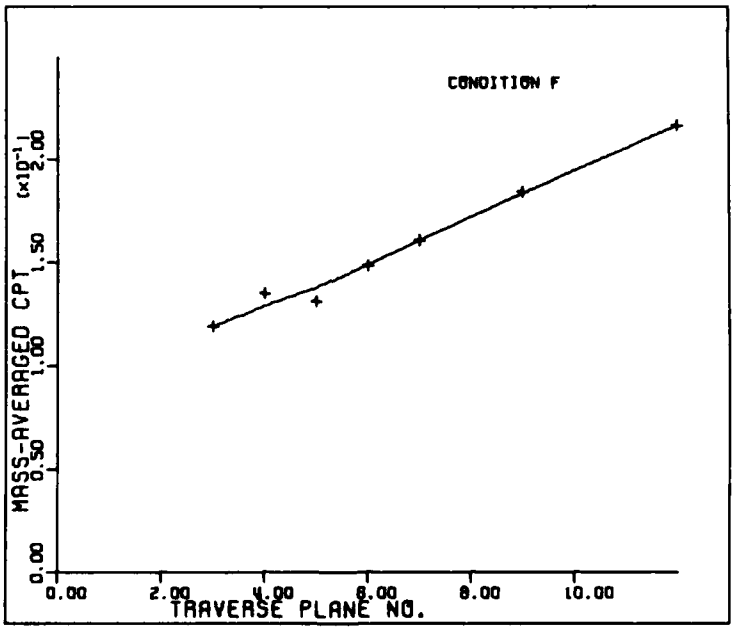

TEST CASE F

Figure 1. (concluded)

increase with the inlet endwall boundary layer momentum thickness, thus accounting for the sharp increases observed in the loss curves.

The accuracy of the mass-weighting integration procedure was verified by comparing the percentage variation in the determined mass flow from traverse plane to traverse plane. The mass flow variation was found to lie within ±3%, indicating good consistency in the probe measurements and in the mass-weighting integration procedures.

Secondary Loss Generation and Loss Migrations

To map out the details of the three-dimensional flow in the passage, computer plots were made of reduced data for the traverse planes measured in the four test cases. Contour plots of locally mass-weighted total pressure coefficients, Cptm, are presented so that loss regions may be identified in the traverse planes and the migration of low momentum fluid through the passage followed.

Figure 2 shows contour plots of Cptm for selected traverse planes in Test Case D ($\theta^*_{inlet}/H = 0.0045$). Figures 3 through 5 also show Cptm contours but for the four test cases compared in Traverse Planes 4, 9, and 12, respectively. For all of the plots shown, the same uniform distribution of contour levels is used, with higher levels indicating higher local total pressure deficit referenced to inlet total pressure. The contour plots are viewed from downstream of the traverse planes, with the suction sidewall (or inside of the passage bend) at the left. Because of symmetry about

midspan, only the lower half of the traverse planes is shown. A consistent qualitative picture of the locally mass-averaged loss behavior throughout the passage can be observed. In the early traverse planes (Traverse Planes 2 and 4) high loss levels are only found in the suction sidewall corner, indicating that the cross flow of the endwall boundary layer has already swept a significant amount of low-momentum fluid into the suction sidewall corner. The plots for succeeding traverse planes show the further accumulation of low-momentum fluid in the suction sidewall corner and the interaction between the endwall and suction sidewall boundary layers. These boundary layers consequently separate to form the passage vortex. As the flow progresses through the passage, the passage vortex can be seen in Traverse Planes 8 through 12 to grow and move up the suction sidewall toward midspan. Essentially, between Traverse Planes 8 and 9, the sidewall boundary layer separates over the complete span. In the remaining planes, the high-loss regions of the passage vortex can be identified, as well as the growth of the vortex and its movement up the suction sidewall. These plots indicate diffusion of the passage vortex and its mixing out with the main flow.

In Figure 5 (for Traverse Plane 4) all Cptm contours show the endwall boundary layer build-up in the suction sidewall corner. Higher loss contours are indicated for Test Case F ($\theta^*_{inlet}/H = 0.022$) than for Test Case D ($\theta^*_{inlet}/H = 0.0045$), but the losses are still characteristic of the collateral inlet boundary layer. In Figure 4, which is for Traverse Plane 9, the passage vortex has formed and is

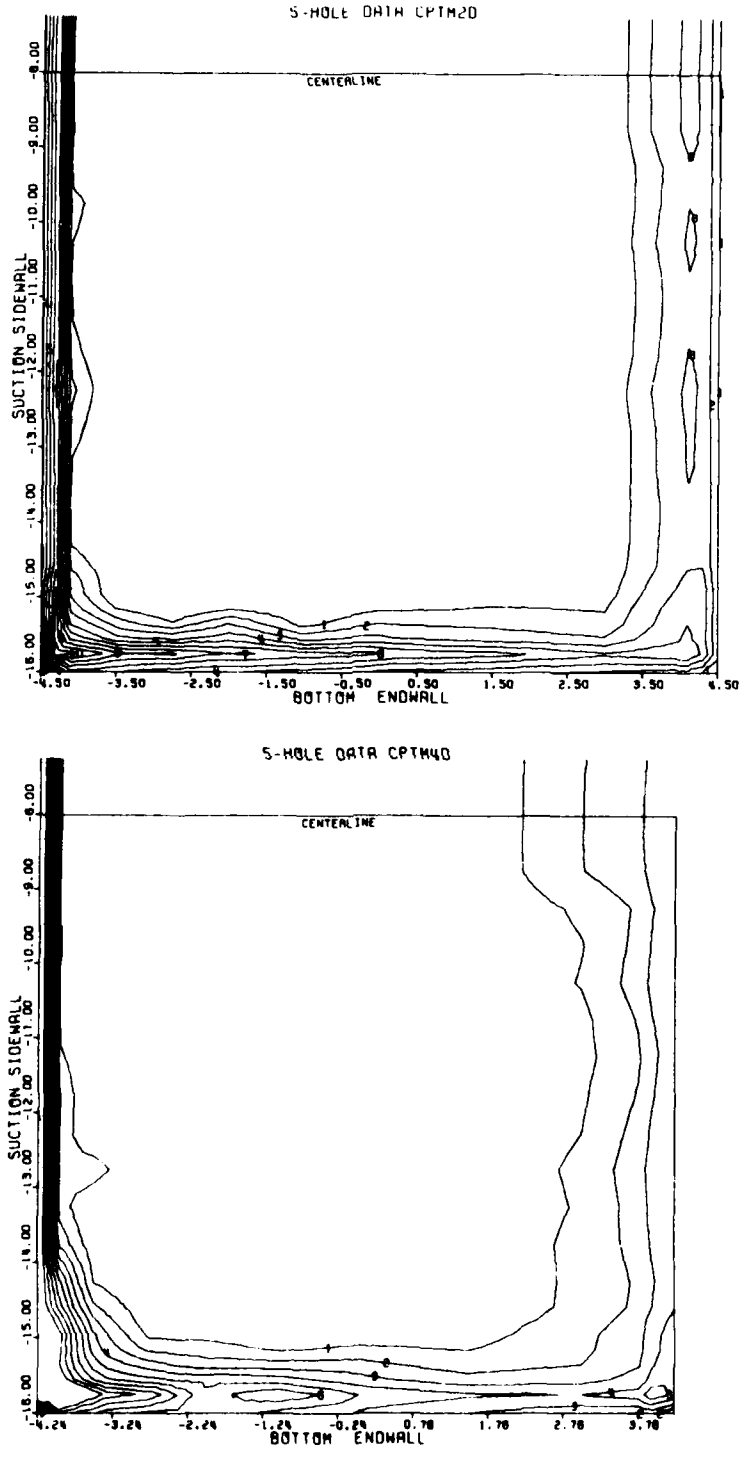

Figure 2. Local mass-weighted total pressure coefficient for selected traverse planes from Test Case D.

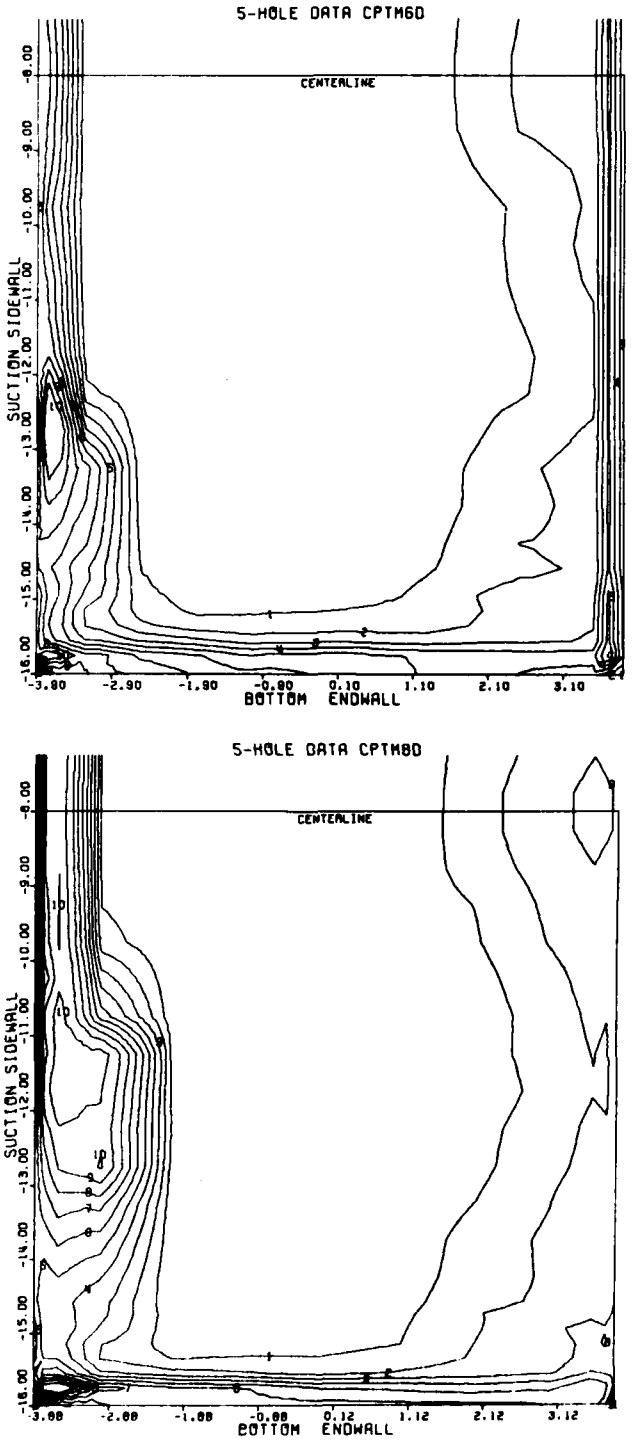

Figure 2. (continued)

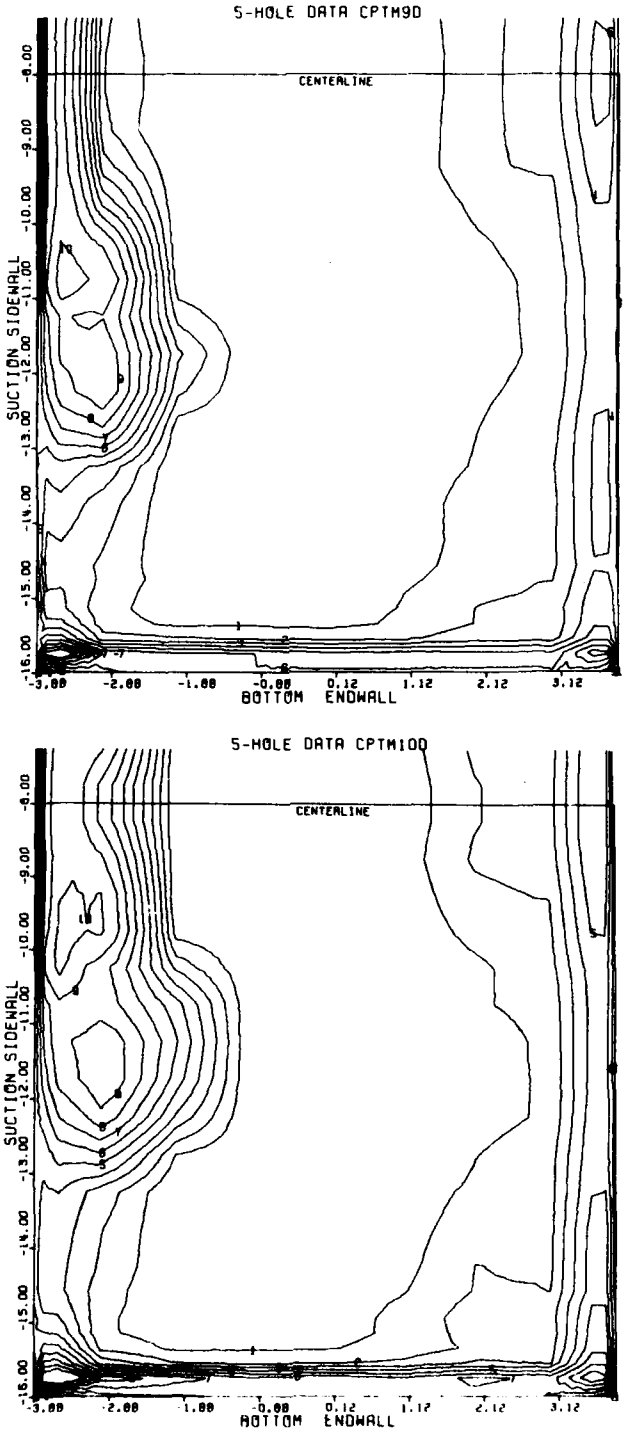

Figure 2. (continued)

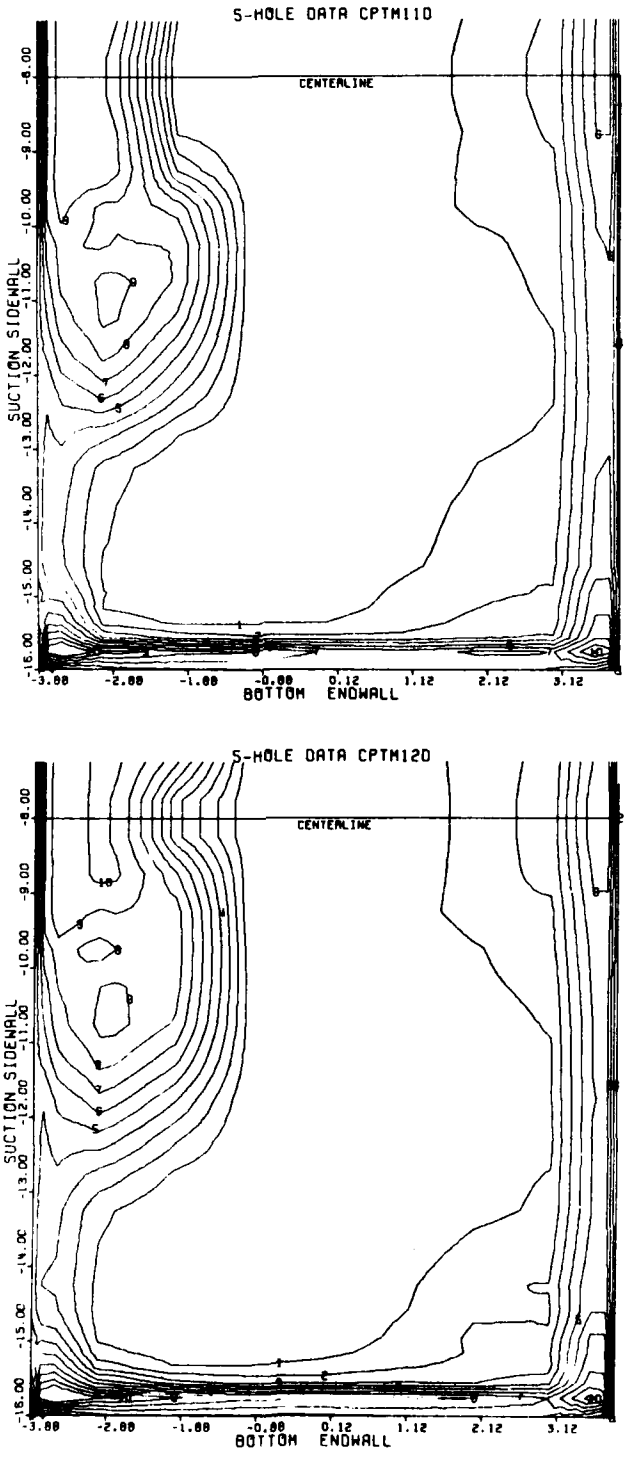

Figure 2. (concluded)

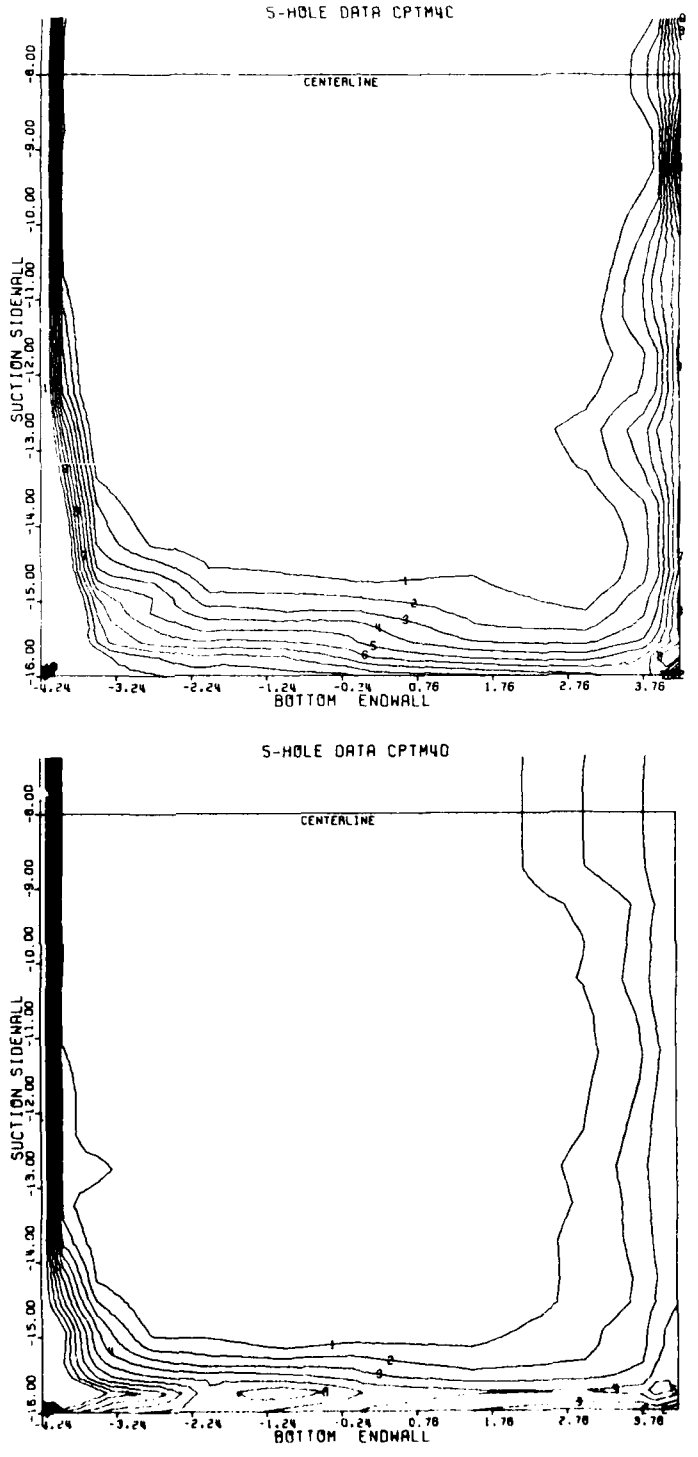

Figure 3. Local mass-weighted total pressure coefficient for Traverse Plane 4 for the four test cases.

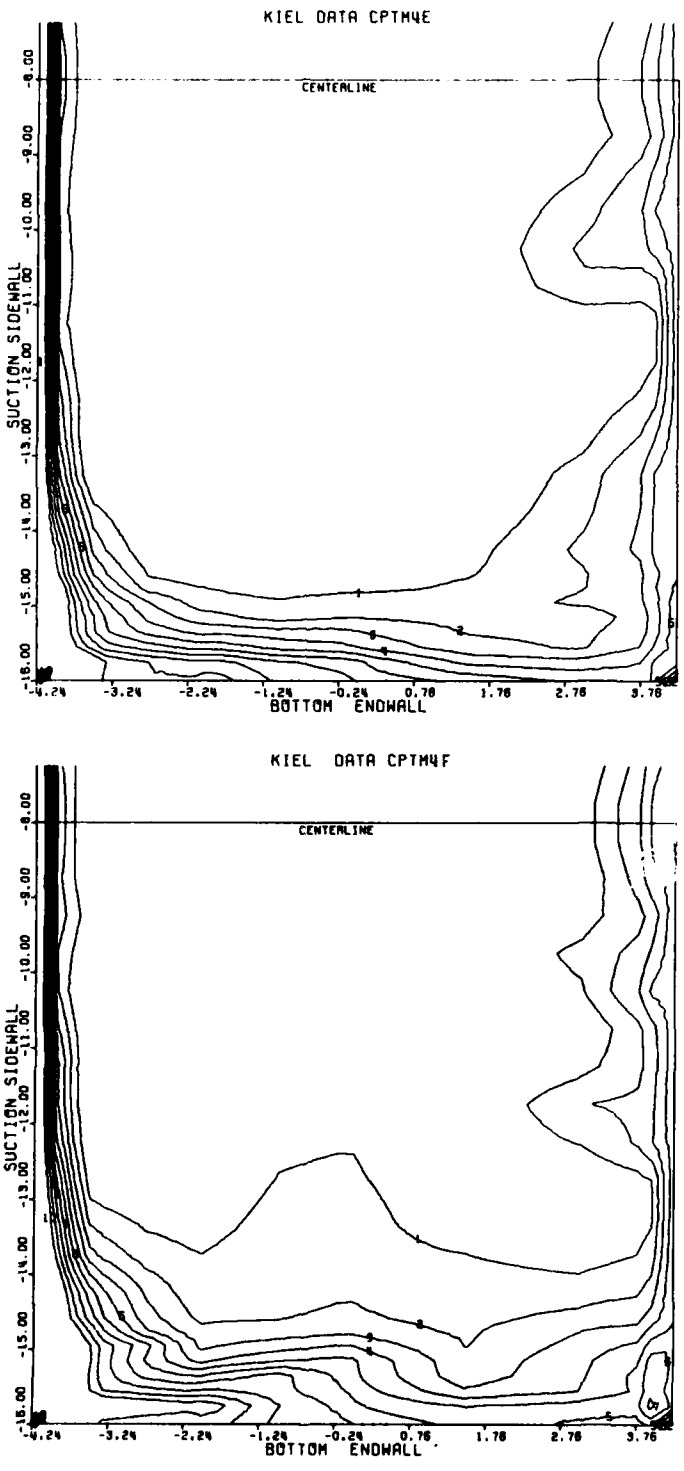

Figure 3. (concluded)

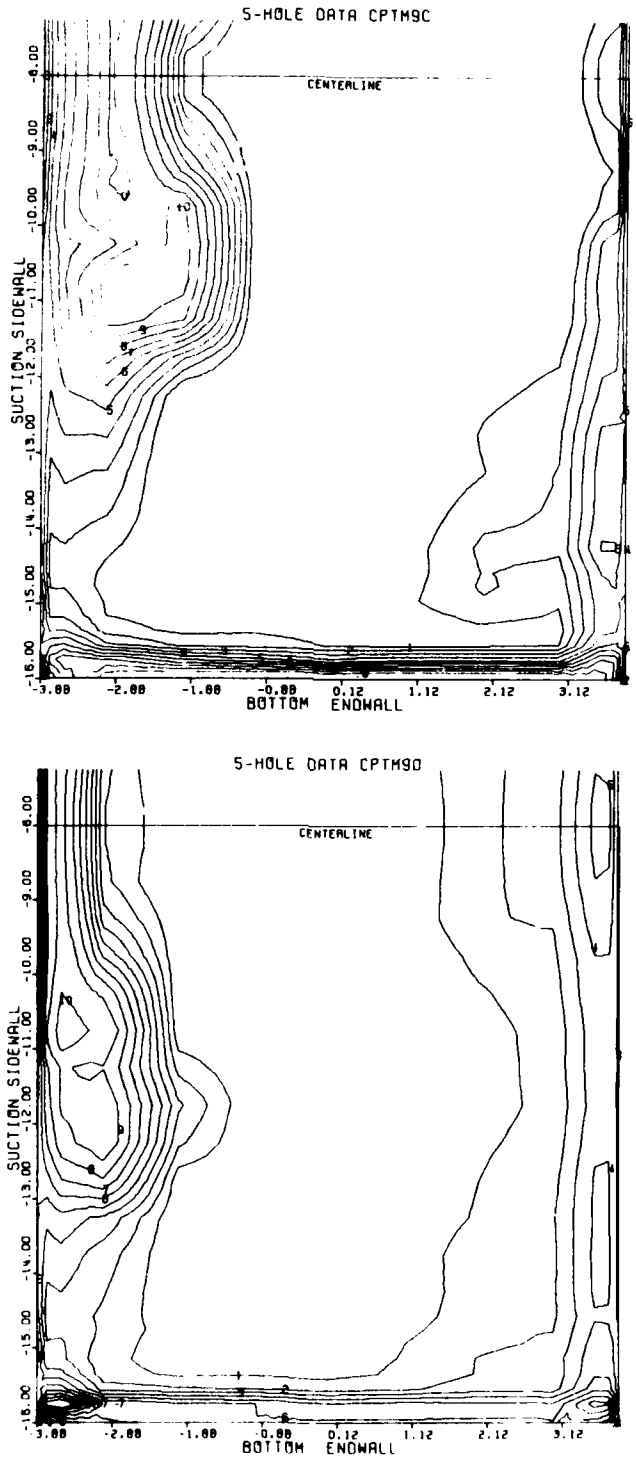

Figure 4. Local mass-weighted total pressure coefficient for Traverse Plane 9 for the four test cases.

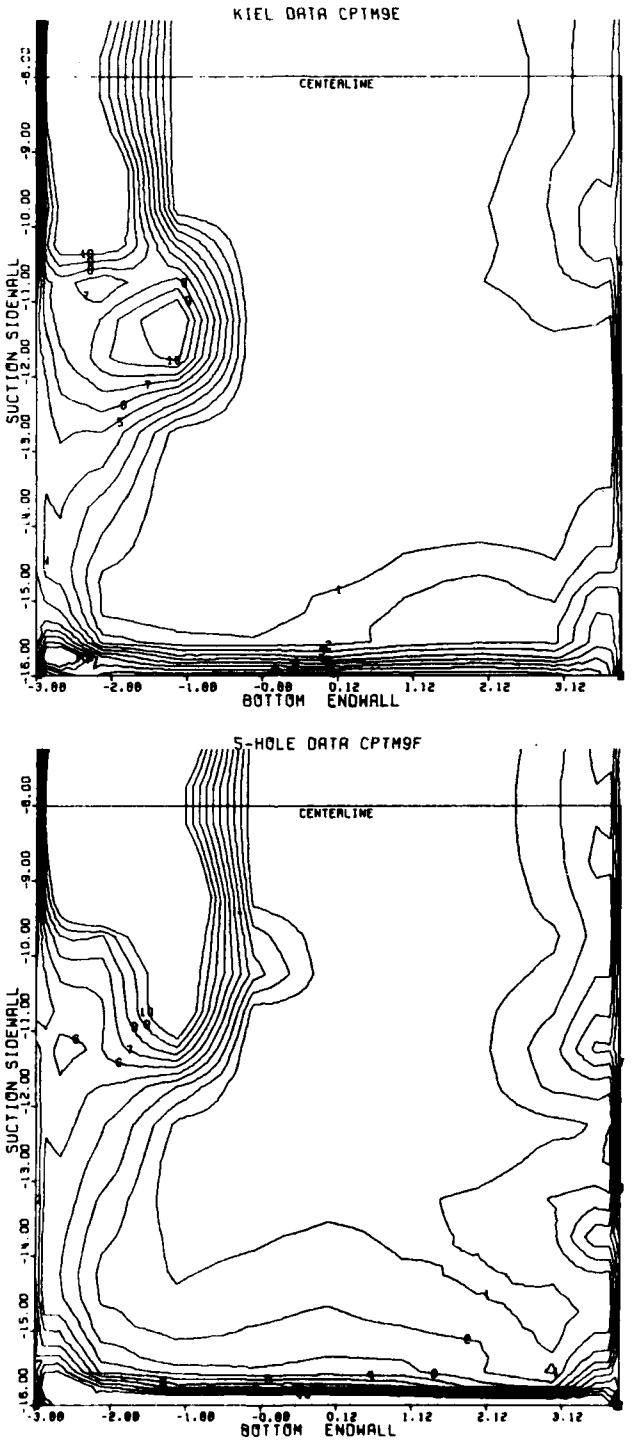

Figure 4. (concluded)

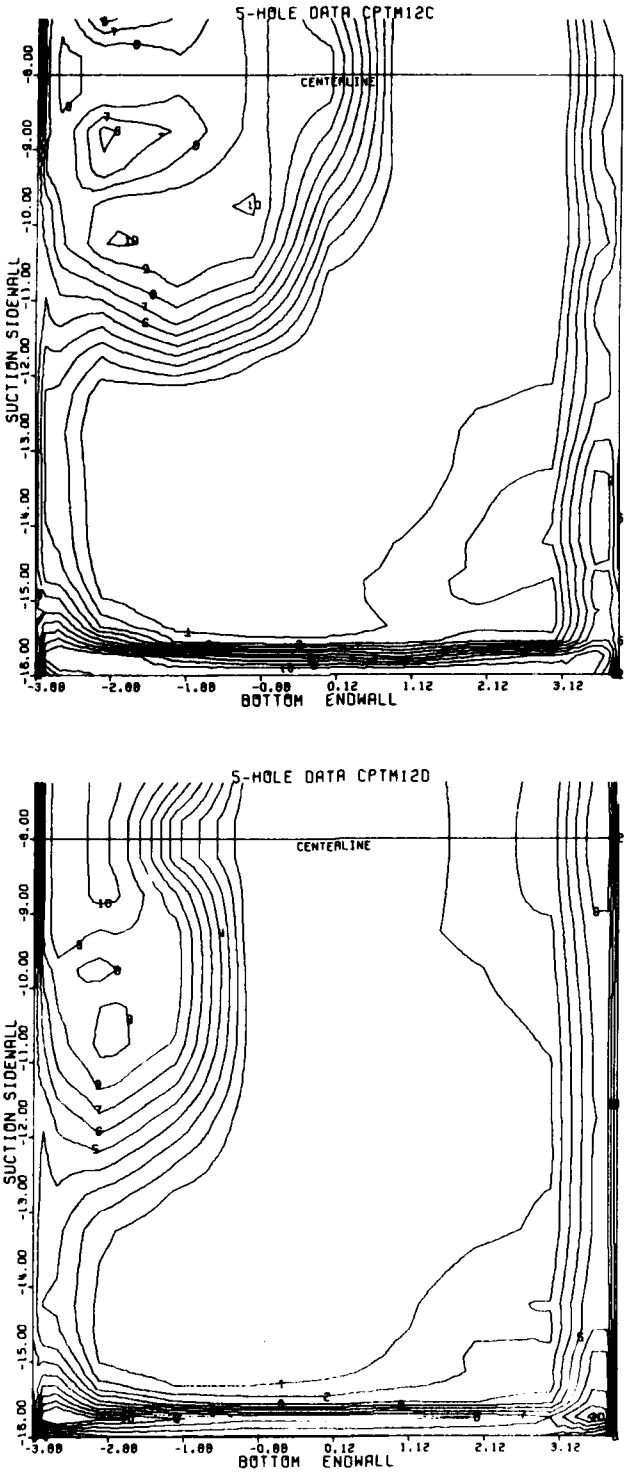

Figure 5. Local mass-weighted total pressure coefficient for Traverse Plane 12 for the four test cases.

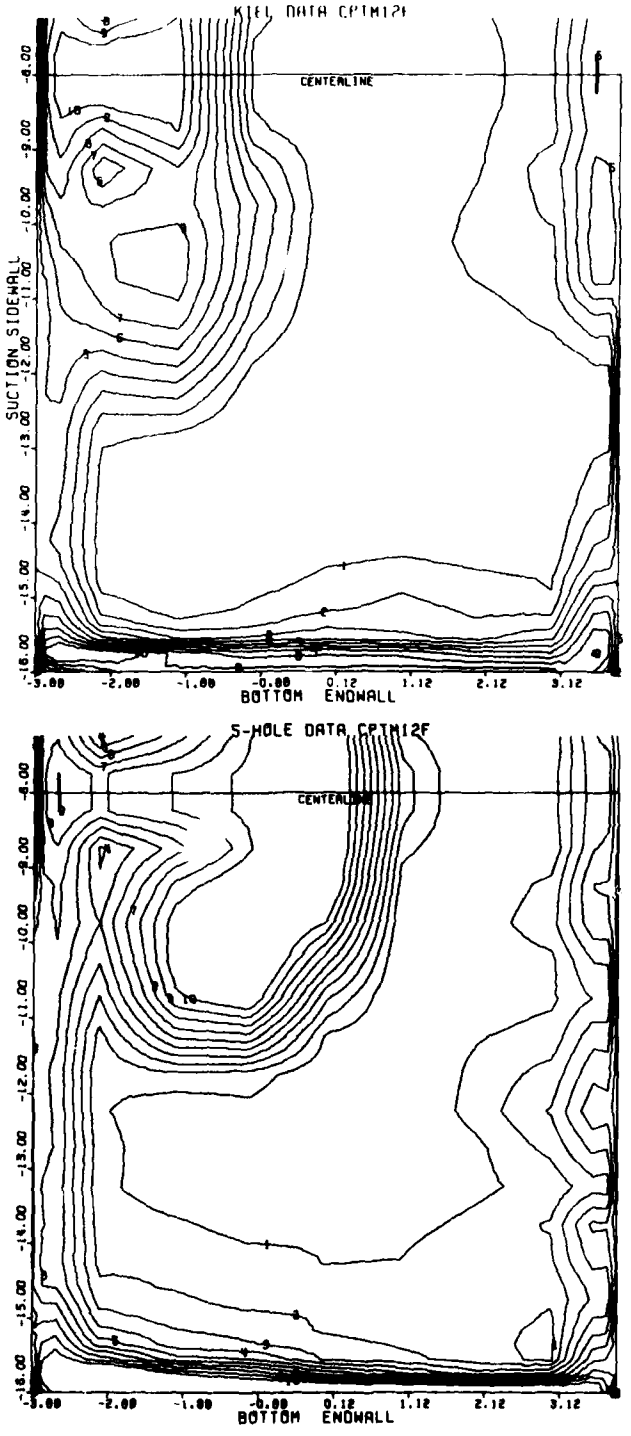

Figure 5. (concluded)

in various stages of development for the different test cases. However, in order of increasing inlet endwall boundary layer momentum thickness, the passage vortex becomes stronger and pushes away from the suction sidewall out into the primary flow towards midspan. In Figure 5, the passage vortex is shown in the exit Traverse Plane 12 for all test cases. Again, the relationship between the inlet endwall boundary layer momentum thickness and the size and location of the passage vortex is evident.

The changes in the locally mass-weighted total pressure coefficient, Cptm (denoted as ΔCptm), from one traverse plane to the next are presented in Figure 6 for Test Case D. From these plots, the migration of low-momentum fluid, and hence losses, through the passage can be observed. The ΔCptm was obtained by calculating the difference in Cptm from traverse plane to traverse plane. Again, similar to contour levels in the previous plots, a uniform distribution of local values of ΔCptm is used. The ΔCptm between Traverse Planes 1 and 2 and between 2 and 3 indicates a total pressure increase in the boundary layer on the pressure sidewall and a decrease on the suction sidewall corresponding to the respective decelerations and accelerations in these regions. ΔCptm contours in the endwall region indicate decreases in the total pressure caused by the endwall crossflow in the earlier traverse planes as it sweeps the low-momentum inlet endwall boundary layer fluid into the suction sidewall corner. The ΔCptm contours for the next several traverse planes in Figure 6 indicate movement of the low total pressure center on the endwall toward the suction sidewall corner. Following the low total pressure center, a higher total

pressure region can be seen, indicating the growth of a new endwall boundary layer. Development of the passage vortex is seen in the plots of ΔCptm between Traverse Planes 6 and 7, and between 7 and 8. Arrows have been added to the ΔCptm plots to help identify specific regions of fluid movement from plane to plane. These point out the movement of the low and high total pressure fluid in the inlet endwall boundary layer which can be seen to move across the endwall, up the suction surface, and into the passage vortex.

Combined results of five-hole probe and hot film measurements extending close to the endwall are presented in Figure 7 for selected probe passes in Traverse Plane 7. The ratio of in-plane or crossflow component u_n to midspan velocity u_m is plotted as a function of spanwise position from the endwall. At the pressure side of the passage, the crossflow is observed to be small; it then increases as the suction side is approached. Close to the suction side in the vicinity of the passage vortex, a crossover crossflow profile is observed. For the probe traverse closest to the suction side where the endwall flow is approaching separation, the positive crossflow again decreases. Figure 8 shows plots of yaw angle deviation in the endwall flow for the same probe traverses discussed in Figure 7. The yaw angle deviation, which is a useful parameter in dealing with three-dimensional boundary layers, is determined by the tangent of the ratio of the local crossflow and throughflow velocity components. Again, due to the small crossflow near the pressure side of the passage, the yaw deviation is small. As the suction side is approached, the strong skewing of the endwall boundary layer and crossover behavior further

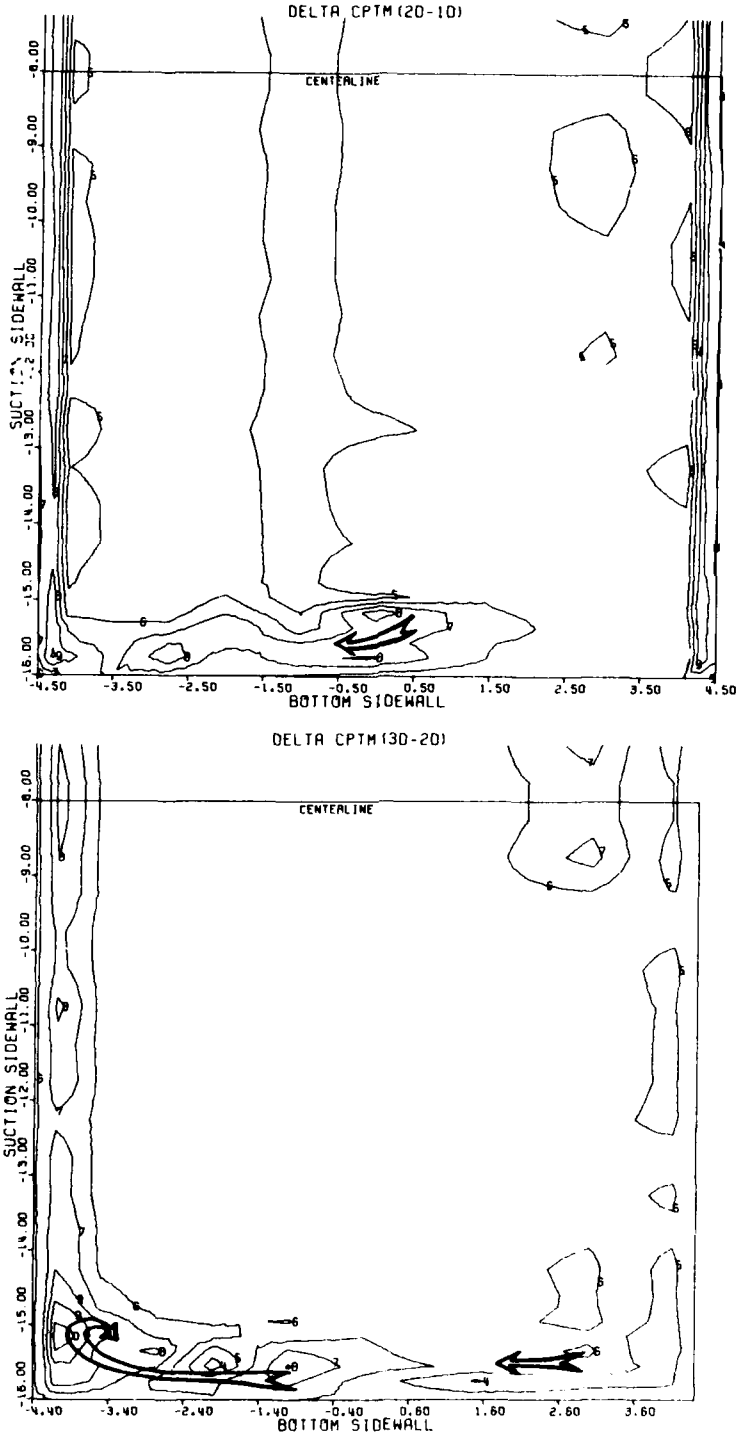

Figure 6. Change in total pressure coefficient relative to previous traverse plane for selected traverse planes from Test Case D.

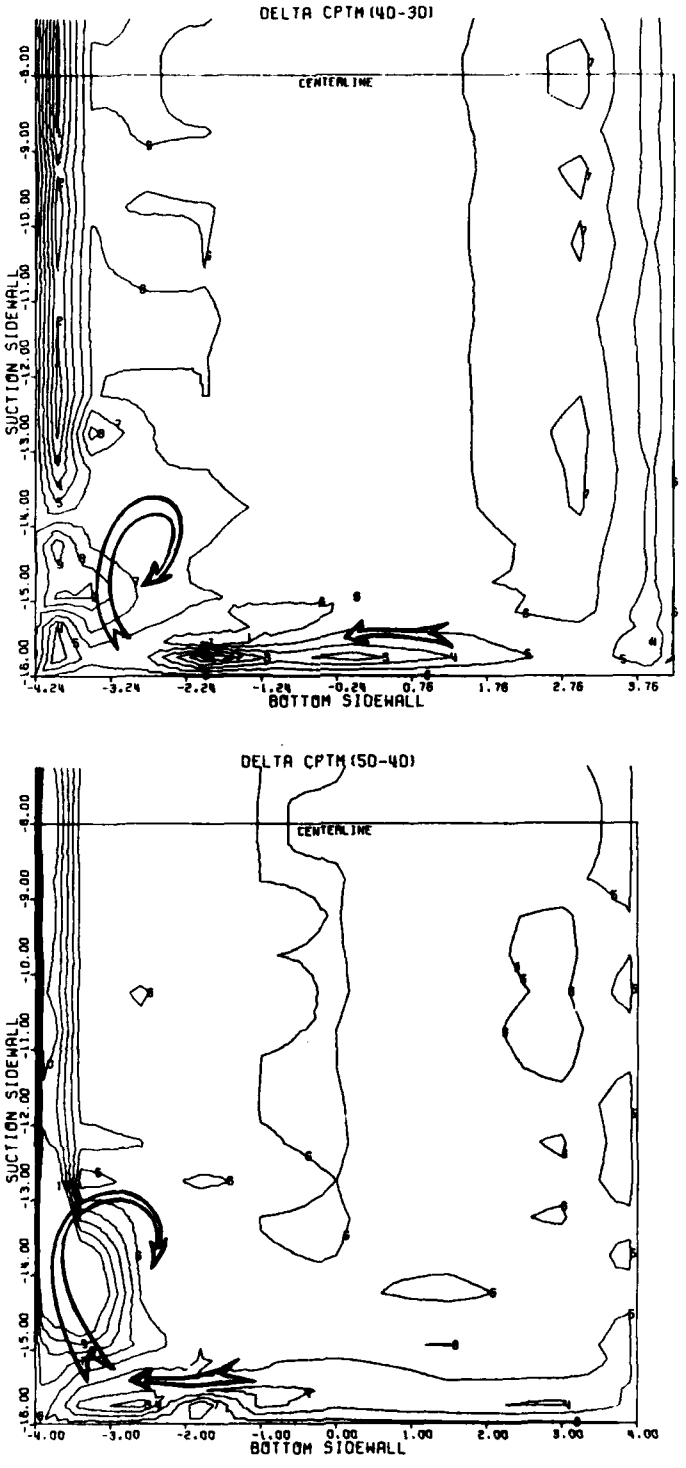

Figure 6. (continued)

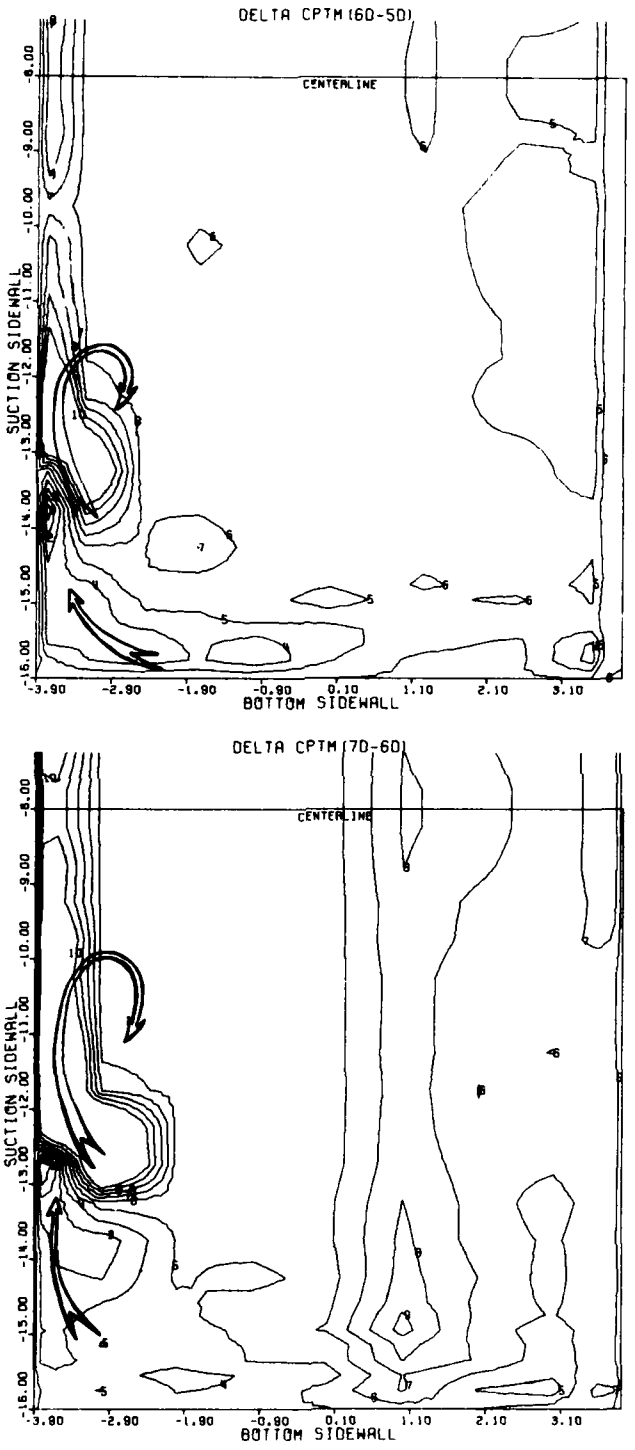

Figure 6. (continued)

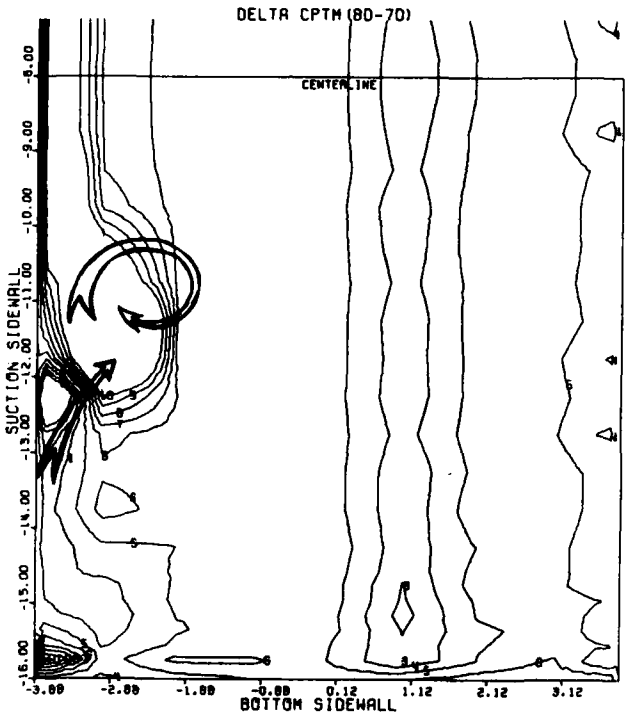

Figure 6. (concluded)

out from the wall are evident. Yaw deviation at the endwall approaches 30 deg. near the pressure side of the passage vortex. A comparison with a quantitative model proposed by Langston [15] based on his cascade data is shown by dashed curve for one of the traverses in Figure 8. The agreement is fairly good, with the present data generally showing less skewing in the immediate vicinity of the endwall.

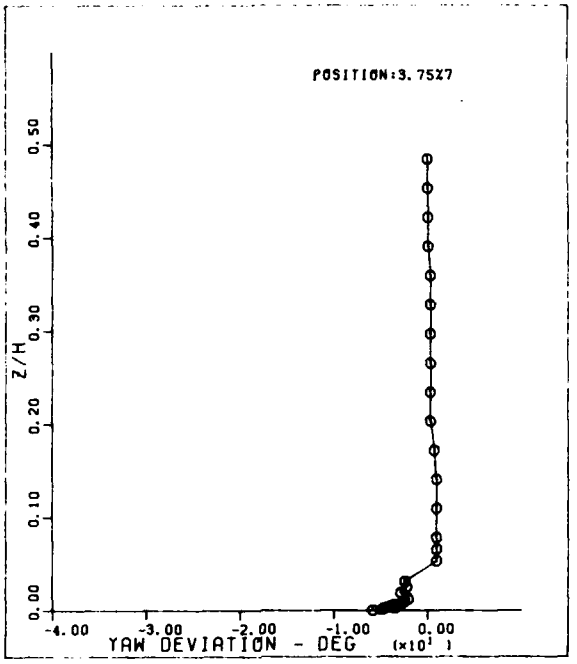

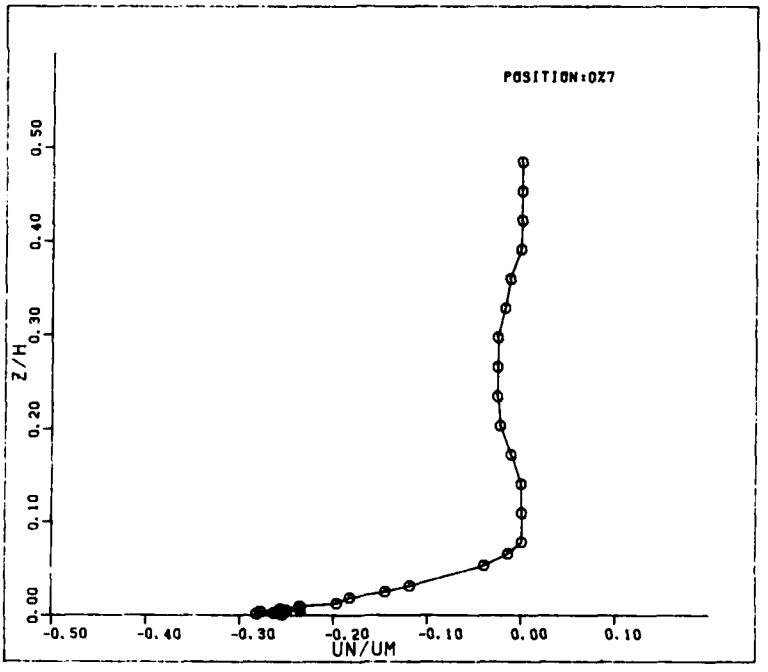

Figure 7. Crossflow variation for four probe traverses in Traverse Plane 7 for Test Case D. Traverse locations are at pressure side, intermediate, and at suction side.

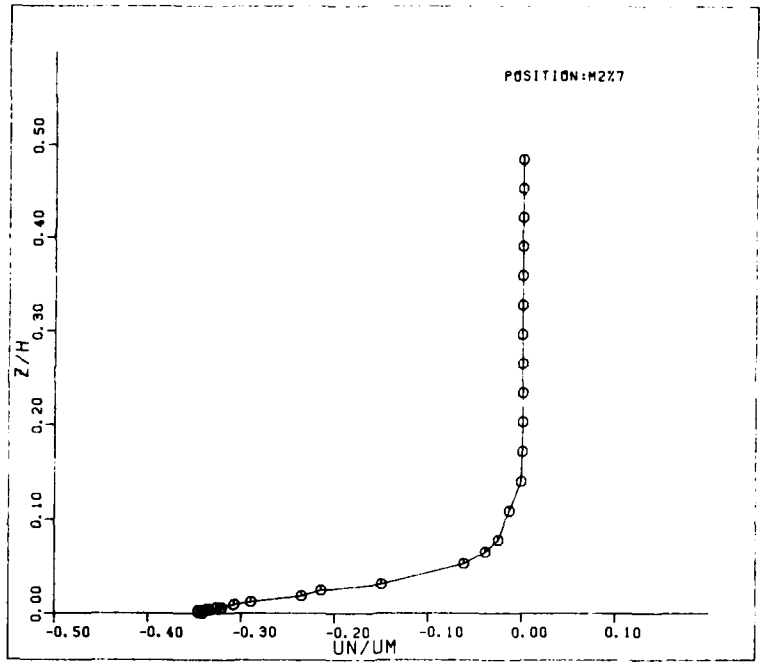

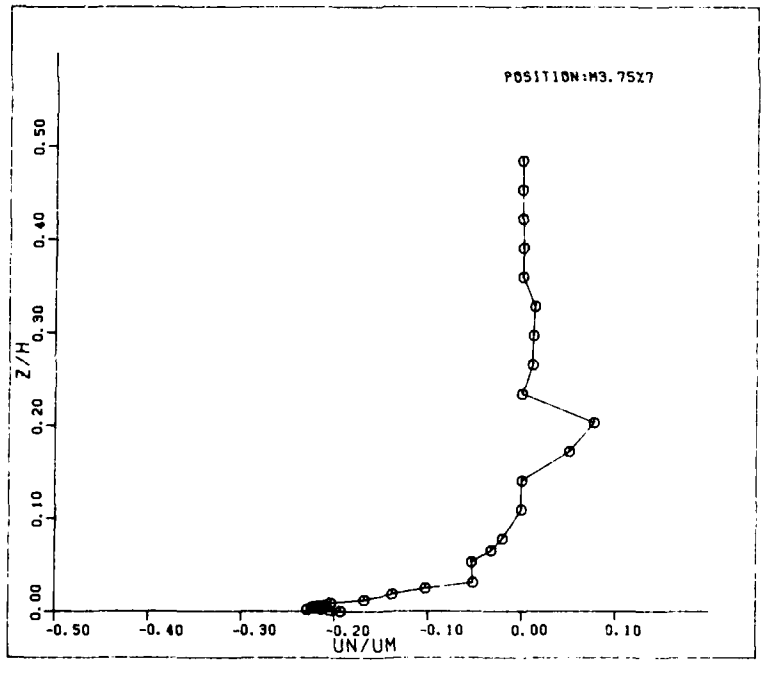

Figure 7. (concluded)

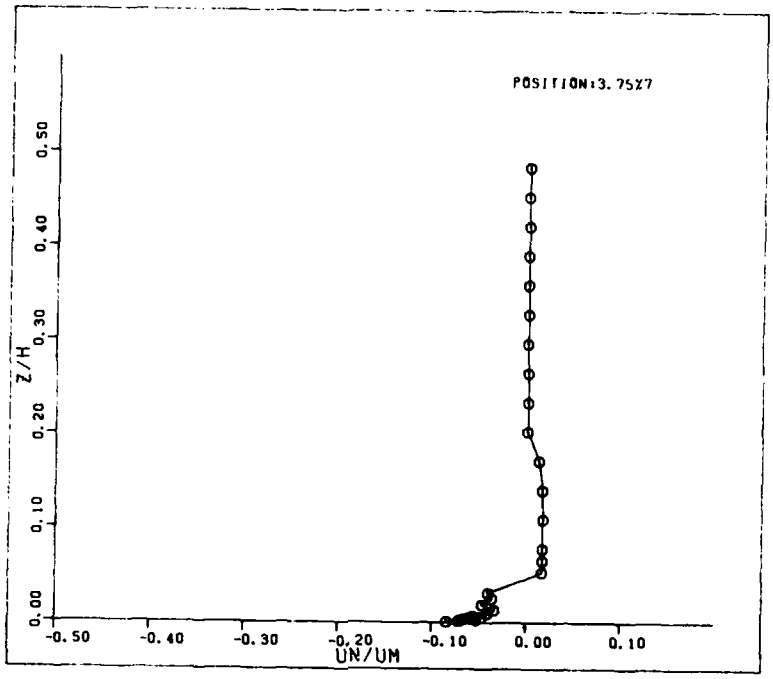

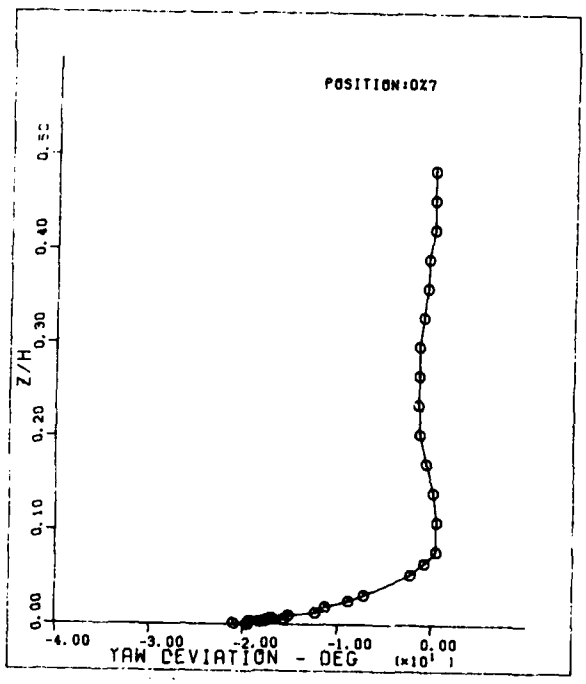

Figure 8. Yaw angle deviation for four probe traverses in Traverse Plane 7 for Test Case D. Traverse locations are at pressure side, intermediate and at suction side.

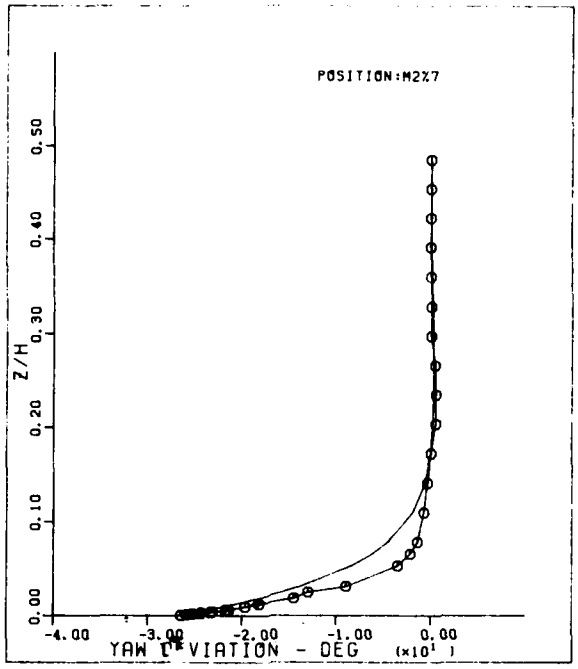

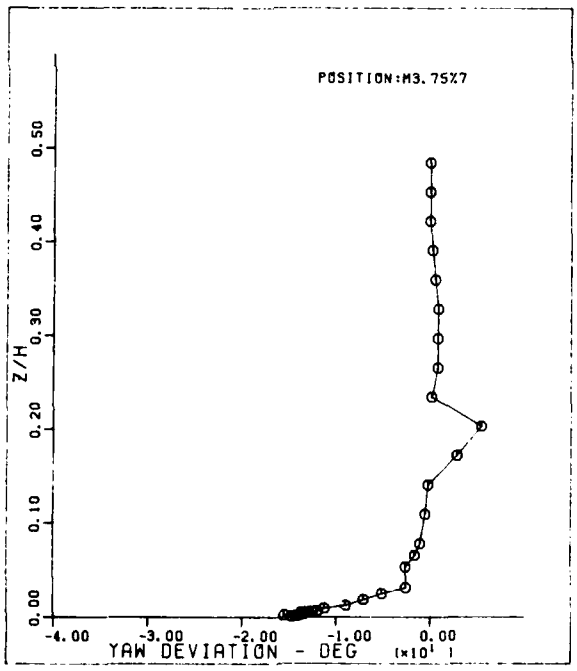

Figure 8. (concluded)

TASK II: EXPERIMENTAL STUDY OF STATOR GEOMETRY MODIFICATIONS FOR IMPROVEMENT OF AXIAL-FLOW COMPRESSOR AERODYNAMIC PERFORMANCE

Introduction

This portion of the research effort involved the overall and detailed performance testing of four two-stage axial-flow compressor builds consisting of baseline rotor blade rows and two kinds of stator blade rows--baseline and modified.

The rotor and baseline stator blades were designed to represent typical transonic compressor stages. Characteristics include high stage reaction, axial flow at the stator exit, and the absence of inlet guide vanes. The double circular arc blade sections used were considered conventional and appropriate for the low-speed testing involved.

The modified stator blades featured forward symmetrical sweep of each stator leading edge from midspan out to inner and outer annulus walls. Past experience [20,21] suggests that modifying a stator blade in this way could result in better flow management in the blade endwall corners.

Some compressor design data are summarized in Table II, and a meridional plane view of the four builds is shown in Figure 9. Several observations about the geometrical aspects of the two stator configurations are noted in Table III in terms of similarities and differences. In Table IV the four compressor builds are compared.

Overall performance data were acquired over the range of compressor flow rates possible in the available test unit and included rotating

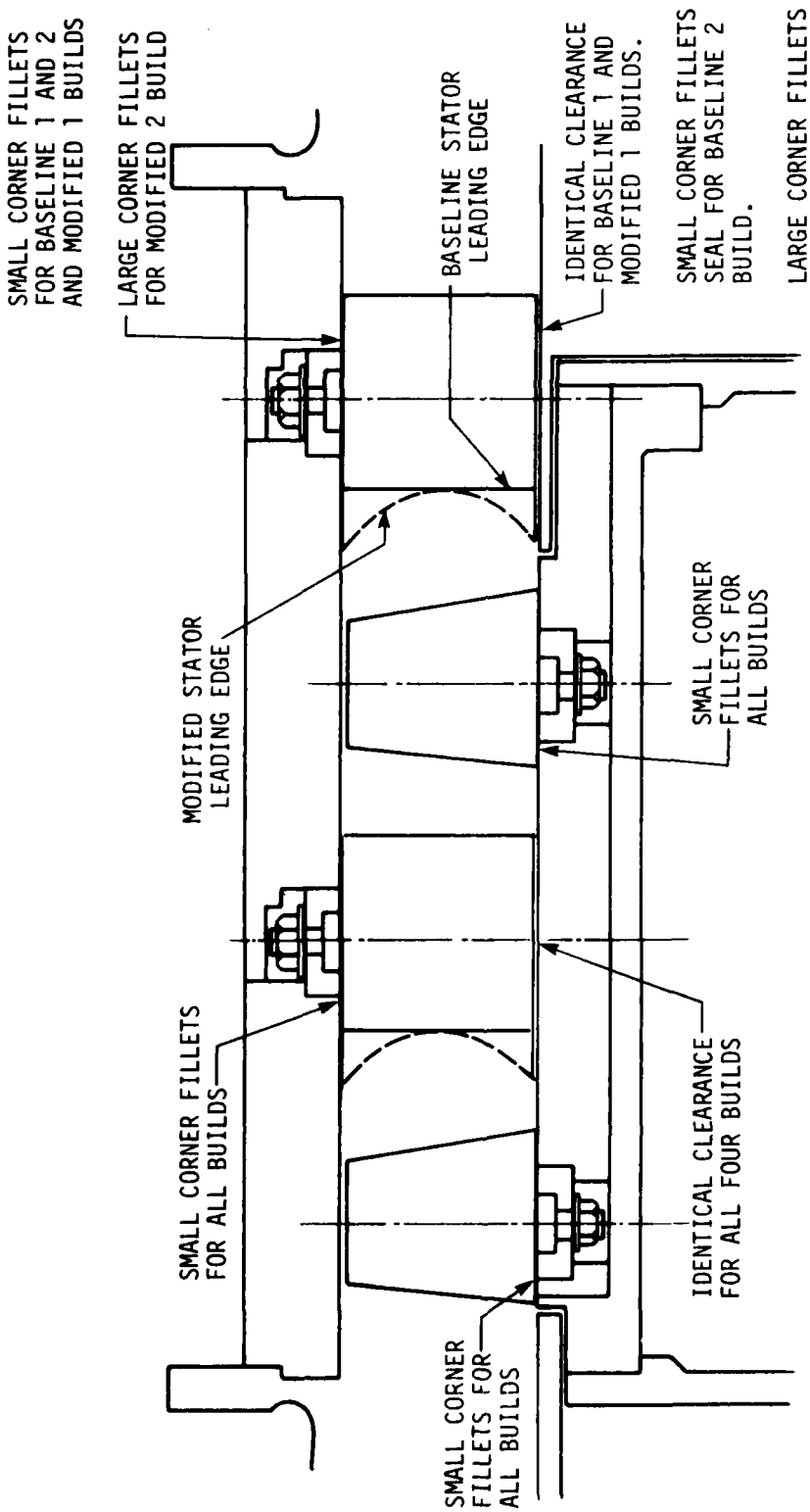

Figure 9. Meridional plane view of four compressor builds.

Table II. Summary of two-stage compressor design data.

Rotor speed	2400 rpm
Flow rate	5.25 lb_m/s (2.38 kg/s)
Pressure ratio	1.019
Number of blades	
Rotor	21
Stator	30
Blade material	fiberglass (steel trunnion)
Blade chord	2.39 in. (6.07 cm) constant for rotor and baseline
	2.38 in. - 3.03 in. (6.04-7.7 cm) for modified stator
Blade profile	double circular arc
Flow path	
Hub radius	5.60 in. (14.22 cm) constant
Tip radius	8.00 in. (20.32 cm) constant

Table III. Comparison of stator blade geometries.

Similarities Between Baseline and Modified Stator Blades	
Number of blades per row	
Blade surface finish	
Mid-span chord length	
Spanwise distribution of maximum thickness to chord ratios	
Differences Between Baseline and Modified Stator Blades	
Baseline	**Modified**
Stacking point at center of gravity	Stacking point at trailing edge circle center
No leading edge sweep	Symmetrical loading edge forward sweep
Constant spanwise distribution of chord length	Varying spanwise distribution of chord length

Table IV. Comparison of compressor builds.

Baseline 1	Baseline 2	Modified 1	Modified 2
Baseline rotor blade rows	Baseline rotor blade rows	Baseline rotor blade rows	Baseline rotor blade rows
Small corner fillets at inner endwall for first and second stage rotor blade rows	Small corner fillets at inner endwall for first and second stage rotor blade rows	Small corner fillets at inner endwall for first and second stage rotor blade rows	Small corner fillets at inner endwall for first and second stage rotor blade rows
Clearance between first stage stator blade tips and rotating inner endwall	Clearance between first stage stator blade tips and rotating inner endwall	Clearance between first stage stator blade tips and rotating inner endwall	Clearance between first stage stator blade tips and rotating inner endwall
Clearance between second stage stator blade tips and stationary inner endwall	Shrouded second stage stator--small corner fillets at inner endwall	Clearance between second stage stator blade tips and stationary inner endwall	Shrouded second stage stator--large corner fillets at inner endwall

stall operation. Complete detailed performance tests were conducted at two flow coefficients only, the design value and one selected to illustrate improvement of total-head rise performance by the modified stator. Some qualitative detailed data were acquired for a range of flow rates.

Highlights of the compressor tests are discussed presently. Related details are included in References 22 and 23.

Baseline Compressor Observations

Analysis of the Baseline 1 build test results for design flow coefficient (0.587) operation led to several important conclusions.

Some limitations of the compressor design procedure used to determine the baseline configuration were observed. Rotor and stator blade section loss estimates were based on a correlation method (Reference 24) that is widely adopted. The differences between measured and design values of rotor and stator loss coefficients suggested the inadequacy of even a state-of-the-art loss prediction method such as the one presently used. Blade deviation angles were estimated for design purposes with a Carter's rule-based procedure [24]. The comparisons between design and actual values of deviation angle demonstrated that rotor section deviation angles could be calculated better than stator angles. A comparison between design and actual velocity triangles showed that serious differences existed between design and actual values of rotor energy addition and downstream stator incidence angles.

Another interesting aspect of the design point operation testing of the Baseline 1 build was the peculiar blade-to-blade total-head distribution observed behind the second stage rotor. Two total-head depressions were present within one stator pitch. The second stage rotor inlet total-head patterns were orthodox, consisting of one total-head depression per stator pitch. The second rotor exit total-head distribution recorded at another flow rate looked "normal," i.e., one total-head depression per stator pitch. Qualitative blade-to-blade total-head survey sketches obtained from photographed oscilloscope traces for 50% span and a variety of flow rates suggested a systematic development of the peculiar two-depression total-head distribution pattern. Heated air tracking of the flow from two adjacent stator blades upstream of the second stage rotor indicated that the two total-head depressions could in fact be identified with freestream and adjacent chopped stator wake avenue portions of flow downstream of the second stage rotor (see Reference 25 for an explanation of the notion of chopped wake avenues). The heated stator wake study revealed that the chopped stator wake avenues are quite wide and actually overlap at low flow rates. Of particular interest were the high total-head regions noted within each wake avenue.

Comparison of Baseline and Modified Stator Performance

Detailed comparison data for the baseline and modified stators were acquired at an operating point associated with a measurable

improvement in total-head rise performance with the modified stator configuration. A flow coefficient of 0.5 was selected.

A graphical comparison of the total-head rise associated with each of the four builds operating at a flow coefficient of 0.5 showed that head-rise gains occurred mainly in the endwall portions of the compressor annulus. The improvement in flow associated with sealing the second stage stator clearance at the stationary inner endwall was substantial. The beneficial effect of leading edge sweep was verified. Large corner fillets at the outer endwall did not result in any observable gain.

Total-head contour plots for the first stator exit flow demonstrated that more high total-head fluid was drawn toward the corner formed by the suction surface of each stator blade and the outer endwall with the modified stators than with the baseline stators. To a lesser extent, the opposite trend was true near the stator pressure surface/outer endwall corner. The differences in contour pattern at the other end of the span of the stator blade, where a clearance was maintained between the stator end and the running rotor hub surface, were less noticeable. Elsewhere along the span the modified stators resulted in wider wakes.

Second stage stator total-head contour plots also indicated that more high total-head fluid was drawn toward the stator suction surface/ outer endwall corner by the modified stator blades than by the baseline stator blades. The opposite trend was repeated near the circumferentially adjacent corner. The influence of large corner fillets at the outer endwall was imperceptible. At the other end of the span of the

stator blade, where a clearance between the stator end and the stationary annulus hub exists, more high total-head fluid was drawn toward the stator suction/inner endwall corner by the modified stator blades than by the baseline stator blades. Sealing the clearance between the stationary hub surface and the stator end eliminated entirely the low total-head fluid region in the suction surface/hub wall corner for both the baseline and the modified stator configurations. Away from the end walls, the modified stators again produced wakes slightly wider than those associated with the baseline stators.

The stator data described above support the idea that sweeping the stator blade leading edge forward in endwall regions of an axial-flow compressor annulus can in effect draw high total-head mainstream fluid toward the lower pressures of the suction surface of the blade's extended portion with resultant benefits. As described in Reference 20, this idea was similarly successful in a linear cascade (leading edge sweep involved about 30% normal chord forward extension over only 8% span length from endwall) and in a low-speed compressor (rotor and stator blades involved leading edge sweep with 13% normal chord forward extension over 7% span at outer wall and 20% normal chord forward extension over 10% span at inner wall) even though forward sweeping of the leading edge was confined only to regions very near the endwalls. The suction surface flow benefit with leading edge sweep is most noticeable at the outer annulus wall corner and is least discerned at the inner annulus wall when a clearance above a moving hub exists. If the stator end clearance occurs above a stationary hub, the leading edge forward sweep benefit is substantial.

On the pressure surface of the leading edge extension upstream into the oncoming flow, the higher surface pressures act in effect to push mainstream fluid away. However, this influence was not seriously detrimental to the pressure side boundary layer flow.

In summary, the forward swept stator configuration effectively managed end-wall flows better than a conventional stator. Also, sealing the clearance between stator end and stationary hub endwall is appreciably beneficial.

TASK III: THE INFLUENCE OF BLADE SURFACE BOUNDARY LAYER AND WAKE FLOWS IN DETERMINING THE PERFORMANCE OF AXIAL-FLOW COMPRESSORS AND TURBINES

In this portion of the program a large number of sets of experimental data from linear cascades and from axial-flow compressor and turbine stages were collected and studied. The objective was to determine the important variables affecting the quantitative behavior of the blade surface boundary region flows in cascade and stage geometries, and to determine whether the aerodynamic variable ranges encountered would be likely to produce similar flow field behavior in the two types of experimental configuration. The motivation for the study was the continuing failure of estimated fluid flow angle and relative total pressure loss patterns to agree with those measured in advanced compressor and turbine stage configurations.

The aerodynamic models utilized in almost all compressor and turbine through-flow calculation methods include the assumption of steady and circumferentially-uniform relative flow at each blade row entrance. This has encouraged confidence in the use of linear cascade experimental programs as elements in the compressor and turbine development process. Individual cascade tests are used in optimization of airfoil and cascade geometry for specific applications, and accumulations of cascade test results are used to develop and extend correlations used in design and analysis systems [Reference 26].

During the 1 October 1980 - 30 September 1981 research year, the significance of the influence of "steady-flow" aerodynamic variable groups on linear cascade and stage blade section performance was

studied. At the same time the numerical range of each variable as encountered in typical linear cascade tests and in blade section operation in compressor and turbine stages was determined so that a judgment might be made concerning the extent of similarity to be expected between cascade and stage blade section performance. As indicated in the 1980-1981 Annual Report [Reference 1], three groups of variables appear to be significant, but inadequately studied and frequently not included in data correlations for either cascades or stage blade sections.

The first group includes Reynolds number, turbulence intensity and scale, and surface finish character (roughness, waviness). This variable group has been shown to be very influential in determining fluid turning and loss in cascade performance computation. Limited low speed linear cascade and stage tests results also show this influence [Reference 27]. There are also strong inferences, but little directly measured proof, in multistage compressor tests [e.g., Reference 28] that the effects of these variables should not be neglected. Unfortunately little or no cascade data exist for the ranges of Reynolds number and turbulence parameters encountered in operational multistage compressors and turbines.

The second class of variables which deserve additional study are those connected with the effects of compressibility on compressor and turbine airfoil performance in the high subsonic velocity regions. Almost all current compressor and turbine configurations are designed so that high subsonic, transonic and supersonic regions of velocity exist in the flow path throughout most of the operating envelope of

the turbine engine or other system application. Only a very limited amount of data using acceptable modern facilities and measurement techniques is available for this velocity range [Reference 29].

The third aerodynamic variable class relates to the effects of effective through-flow passage area on blade section performance. In the case of a steady flow through a cascade of airfoil profiles, this reduces to the rate at which average axial velocity × density product changes in the blade-to-blade passage and in the downstream region. This is a very difficult variable to measure and control, but its influence is considerable.

All three of these classes of variables can be satisfactorily accounted for in terms of boundary-layer and wake development. This calls not only for reliable and comprehensive computation and prediction methods, but also for more extensive collection of boundary layer and wake data to support analysis and computation. Throughout the time span of AFOSR Grants 81-0004 and 81-0004A, negotiations have been carried on to allow the acquisition of new linear cascade data on a modern compressor blade section profile. During 1981-1982 agreement was reached on an attractive cascade geometry and on general terms of data acquisition and distribution. A cooperative program including new experiments in facilities of the West German and French aeronautical research agencies DFVLR and ONERA has been developed. The test programs will include experiments on geometrically similar cascade packs with each test group utilizing its state-of-the-art test technique. Data analysis will be carried on jointly, and it is expected that a mutually acceptable set of performance characteristics will emerge.

The data should serve as an example of good experimental procedure and as test case information for comparison purposes.

A group of variables totally unaccounted for in linear cascade testing, but obviously present in compressor and turbine operation, includes those related to unsteady flow. The mechanisms of unsteady flow field development in compressors and turbines range from blade-passing-frequency wake unsteadiness due to an immediate upstream blade row, through more complex blade-wake chopping and transport effects involving several blade rows, to the large-scale unsteadiness of rotating stall, inlet distortion and surge [Reference 30]. During 1981-1982 the unsteadiness at the entrance to a given blade row caused by fluctuations in velocity magnitude and direction due to the wakes of an immediately adjacent upstream blade row were studied in some depth. The objective was to determine whether a means for accomodating this unsteadiness might be included in design and analysis system calculations. It has been noted earlier that the basic aerodynamic model for through-flow calculations assumes steady relative flow. It has also been observed that all correlated linear cascade data derives from steady entrance flow experiments, and that much research on compressor and turbine blade rows occurs in annular cascades and single rotors which minimize unsteadiness. Yet it is obvious that the vast majority of compressor and turbine blades operate in a highly unsteady flow.

Data has been obtained from NASA [Reference 31] and DFVLR [Reference 32] experiments in which detailed compressor rotor flow field data were measured by laser velocimeter systems. These data have been studied to determine the velocity magnitude and direction variations,

and the actual and reduced frequencies associated with typical compressor rotor wake region flows. Numerical values for all of these wake variables verify the need for an unsteadiness allowance in optimizing incidence and in predicting blade row turning and loss.

SECTION III. PUBLICATIONS

The following list includes documents published since October 1, 1980 that are based entirely or in part on research supported by the AFOSR.

1. Hansen, E. C., Serovy, G. K., and Sockol, P. M. Axial-Flow Compressor Turning Angle and Loss by Inviscid-Viscous Interaction Blade-to-Blade Computation. Journal of Engineering for Power, Trans. ASME. 102: 28-34, 1980.
2. Serovy, G. K., Kavanagh, P., and Okiishi, T. H. Aerodynamics of Axial-Flow Turbomachinery. Iowa State University Engineering Research Institute Technical Report TCRL-17, 1980.
3. Zierke, W. C., and Okiishi, T. H. Measurement and Analysis of the Periodic Variation of Total Pressure in an Axial-Flow Compressor Stage. Iowa State University Engineering Research Institute Technical Report TCRL-18, November 1980.
4. Hottman, D. A. Turbomachinery Laboratory Data Acquisition and Experiment Control Systems. Iowa State University Engineering Research Institute Technical Report TCRL-19, 1980.
5. Okiishi, T. H. Periodically Unsteady Flow Through an Imbedded Stage of a Multistage Axial-Flow Turbomachine. In Aeroelasticity of Turbine Engines, Joint NASA/AF/Navy Symposium Preprint, October 1980.
6. Serovy, G. K., and Hansen, E. C. Computation of Flow in Radial- and Mixed-Flow Cascades by an Inviscid-Viscous Interaction Method. In Centrifugal Compressors, Flow Phenomena and Performance, AGARD-CP-282, 1980.

7. Smith, P. G. Calibration of Five-Hole Directional Pressure Probes. Iowa State University Engineering Research Institute Technical Report TCRL-20, 1980.

8. Serovy, George K., and Bry, Pierre. Loss Distributions in Axial-Flow Compressor Blade Rows. International Symposium on Applications of Fluid Mechanics and Heat Transfer to Energy and Environmental Problems. University of Patras, Patras, Greece, June 1981.

9. Serovy, George K. Deviation/Turning Angle Correlations. In Through Flow Calculations in Axial Turbomachines. AGARD Advisory Report 175, 1981, pp. 184-211.

10. Serovy, George K. Axial-Flow Turbomachine Through-Flow Calculation Methods. In Through Flow Calculations in Axial Turbomachines. AGARD Advisory Report 175, 1981, pp. 285-305.

11. Kluck, C. E. Prediction of Laminar-to-Turbulent Boundary Layer Transition in Axial-Flow Turbomachinery. Iowa State University Engineering Research Institute Technical Report TCRL-21, 1981.

12. Serovy, G. K., Kavanagh, P., and Okiishi, T. H. Aerodynamics of Advanced Axial-Flow Turbomachinery. Iowa State University Engineering Research Institute Technical Report TCRL-22, 1981.

13. Zierke, W. C., and Okiishi, T. H. Measurement and Analysis of Total-Pressure Unsteadiness Data from an Axial-Flow Compressor Stage. Journal of Engineering for Power, Trans. ASME. 104: 479-488, 1982.

14. Serovy, G. K., Kavanagh, P., and Okiishi, T. H. Aerodynamics of Advanced Axial-Flow Turbomachinery. Iowa State University Engineering Research Institute Technical Report TCRL-23, 1983.

15. Hathaway, M. D., and Okiishi, T. H. Aerodynamic Design and Performance of a Two-Stage, Axial-Flow Compressor (Baseline). Iowa State University Engineering Research Institute Technical Report TCRL-24, 1983.

16. Tweedt, D. L., and Okiishi, T. H. Effects of Stator Blade Row Geometry Modifications on Two-Stage Axial-Flow Compressor Aerodynamic Performance. Iowa State University Engineering Research Institute Technical Report TCRL-25, 1983.

17. Kavanagh, P., McAndrew, J. A., and Shyh, C-K. Experimental Data Compilation for Flow in a Curved Rectangular Cross-Section Passage. Iowa State University Engineering Research Institute Technical Report TCRL-26, 1983.

18. Serovy, George K. Present Status of Aerodynamic Loss Distribution Measurement and Prediction for Axial-Flow Compressors and Turbines. Iowa State University Engineering Research Institute Technical Report TCRL-27, 1983.

SECTION IV. PROGRAM PERSONNEL

Three principal investigators share responsibility for the current program.

- George K. Serovy, Anson Marston Distinguished Professor in Engineering, Tasks II and III
- Patrick Kavanagh, Professor of Mechanical Engineering, Task I
- Theodore H. Okiishi, Professor of Mechanical Engineering, Task II

Six graduate-level engineers have also been associated with the work.

- John A. McAndrew, Graduate Research Assistant, Task I
- C-K. Shyh, Graduate Research Assistant, Task I
- Michael D. Hathaway, Graduate Research Assistant, Task II
- Daniel L. Tweedt, Graduate Research Assistant, Task II
- William C. Zierke, Graduate Research Assistant, Task II
- Ruth A. Spear, Graduate Research Assistant, Task III
- James A. Parsons, Graduate Research Assistant, Task III

During the research several undergraduate students in Mechanical Engineering have made useful contributions. This is an effective mechanism for introducing undergraduates to the research activity in turbomachinery.

- Keith A. Dau-Schmidt, Undergraduate Assistant, Task I
- Mark T. Diefenthaler, Undergraduate Assistant (to 1 March 1981), Task I

- Douglas A. Hottman, Undergraduate Assistant (to 1 December 1980), Task I
- Gregory R. Palczewski, Undergraduate Assistant, Task I
- Paul G. Smith, Undergraduate Assistant (to 1 March 1981), Task I
- Robert A. Uhlig, Undergraduate Assistant, Task I
- Gary P. Campbell, Undergraduate Assistant, Task II
- Jeff L. Hansen, Undergraduate Assistant, Task II

SECTION V. INTERACTION WITH UNITED STATES AND FOREIGN GOVERNMENT AGENCIES AND INDUSTRY

The turbomachinery research program at Iowa State University has focused on projects which make a contribution to the development of design systems for advanced compressors, fans, and turbines for air-breathing aircraft propulsion systems. The current grant has not changed this focus and has involved numerous direct contacts with outside organizations.

Tasks II and III depend on substantial cooperation with USAF/AFAPL and industry. A list of the visits and telephone contacts for Task II follows.

Organization and Nature of Contact	Individual Contacts
NASA-Lewis Research Center, Cleveland, Ohio; lab visits and technical discussions	C. Ball J. E. Crouse D. M. Sandercock Dr. A. J. Strazisar
Air Force Aero Propulsion Laboratory, Wright-Patterson Air Force Base, Ohio; technical discussions	Dr. A. J. Wennerstrom
General Electric Company, Advanced Turbomachinery Aerodynamics, Cincinnati, Ohio; discussion of blade fabrication problems	Dr. D. C. Wisler

Organization and Nature of Contact	Individual Contacts
Pratt & Whitney, East Hartford, Connecticut; discussion of blade fabrication problems	H. Weingold
Air Research, Phoenix Division, Phoenix, Arizona; test cases	J. R. Switzer P. Dodge
Institut für Antriebstechnik, Deutsche Forschungs- und Versuchsanstalt für Luft- und Raumfahrt, Köln, West Germany; planning of test program, review of results	Dr. G. Winterfeld Dr. H. Starken Dr. H. B. Weyer
Direction de l'Energetique, Office National d'Etudes et de Recherches Aérospatiales, Châtillon-sous-Bagneux, France; planning of test program	J. Fabri G. Meauzé S. Boudigues
NASA-Lewis Research Center, Cleveland, Ohio; computation, test cases, review of results	D. M. Sandercock T. Gelder
Middle East Technical University, Ankara, Turkey	A. S. Ucer
Free University of Brussels, Brussels, Belgium	C. Hirsch

SECTION VI. DISCOVERIES, INVENTIONS, AND SCIENTIFIC APPLICATIONS

No fundamentally new concepts or devices were developed. However, Task II involved some blade design concepts which originated in AFAPL and may, after further experimental evaluation and development, lead to improved multistage compressor performance.

SECTION VII. CONCLUDING REMARKS

The two-year period covered by AFOSR Grants 81-0004 and 81-0004A was characterized by the accumulation and analysis of experimental data in Tasks I and II, and by the collection and evaluation of outside data for Task III. The technical achievements are summarized in this report and other reports in the Iowa State TCRL series.

The research program on Aerodynamics of Advanced Axial-Flow Turbomachinery has produced a coordinated effort involving faculty, graduate students, and undergraduate assistants. The resulting continuity allows for the development of qualified personnel as well as useful research information.

REFERENCES

1. Serovy, G. K., Kavanagh, P. and Okiishi, T. H. Aerodynamics of Advanced Axial-Flox Turbomachinery. Iowa State University Engineering Research Institute Technical Report TCRL-22, 1981.

2. McAndrew, J. A. Experimental Investigation of Three-Dimensional Flow in a Curved Rectangular Cross-Section Duct. Unpublished M.S. Thesis. Iowa State University. 1982.

3. Shyh, C-K. Experimental Investigation of Endwall Crossflow in a Curved Rectangular Cross-section Duct. Unpublished M.S. Thesis. Iowa State University. 1983.

4. Kavanagh, P., McAndrew, J. A. and Shyh, C-K. Experimental Data Compilation for Flow in a Curved Rectangular Cross-Section Passage. Iowa State University Engineering Research Institute Technical Report TCRL-26, 1983.

5. Herzig, H. Z. and Hansen, A. G. Visualization Studies of Secondary Flows with Applications to Turbomachinery. Transactions American Society of Mechanical Engineers 77: 249. 1955.

6. Herzig, H. Z. and Hansen, A. G. Experimental and Analytical Investigation of Secondary Flows in Ducts. Journal of Aeronautical Sciences 24: 217. 1957.

7. Armstrong, W. D. Secondary Flow in a Cascade of Turbine Blades. Aero. Res. Council Reports & Memoranda No. 2979. 1955.

8. Moore, R. W. and Richards, D. L. Skewed Boundary Layer Flow Near the Endwalls of a Compressor Cascade. Transactions American Society of Mechanical Engineers 79: 1789-1800. 1957.

9. Turner, J. R. An Investigation of the Endwall Boundary Layer in a Turbine Nozzle Cascade. Trans ctions American Society of Mechanical Engineers 79: 1801-1806. 1957.

10. Senoo, Y. The Boundary Layer on the Endwall of a Turbine Nozzle Cascade. Transactions American Society of Mechanical Engineers 80: 1711-1720. 1958.

11. Belik, L. An Approximate Solution for the Kinetic Energy of Secondary Flow in Blade Cascades. International Journal of Mechanical Sciences 10: 765. 1968.

12. Belik, L. Secondary Flow in Blade Cascades of Axial Turbomachines and the Possibilities of Reducing Its Unfavorable Effects. Proceedings - 1972 2nd Japan Society of Mechanical Engineers Symp. on Fluid Machinery and Fluidics 1: 41-49. 1972.

13. Came, P. M. Secondary Loss Measurements in a Cascade of Turbine Blades. The Institution of Mechanical Engineers, Conference Publication 3: 75-83. 1973.

14. Langston, L. S., Nice, M. L., and Hooper, R. M. Three-Dimensional Flow Within a Turbine Cascade Passage. American Society of Mechanical Engineers Paper No. 76-GT-50. 1976.

15. Langston, L. S. Crossflows in a Turbine Cascade. Transactions American Society of Mechanical Engineers 102: 866-874. 1980.

16. Joy, W. Experimental Investigation of Shear Flow in Rectangular Bends. Master of Science Thesis. Massachusetts Institute of Technology, Cambridge, Mass. 1950.

17. Eichenberger, H. P. Shear Flow in Bends. Massachusetts Institute of Technology, Technical Report No. 2. 1952.

18. Bruun, H. H. An Experimental Investigation of Secondary Flow Losses in Bends with Rectangular Cross Sections. Cambridge University. Department of Engineering, Report No. CUED/A - Turbo/TR-95. 1979.

19. McMillan, O. J. Mean Flow Measurements of the Flow Field Diffusing Bend. NASA CR 3634. 1982.

20. Wennerstrom, A. J. and Frost, G. R. Design of a 1500 ft/sec, Transonic, High-Through-Flow, Single-Stage Axial Flow Compressor with Low Hub/Tip Ratio. AFAPL-TR-76-59. 1976.

21. Senoo, Y., Taylor, E. S., Batra, S. K. and Hinck, E. Control of Wall Boundary Layer in an Axial Compressor. Massachusetts Institute of Technology Gas Turbine Laboratory Report Number 59. 1960.

22. Hathaway, M. D. and Okiishi, T. H. Aerodynamic Design and Performance of a Two-Stage, Axial-Flow Compressor (Baseline). Iowa State University Engineering Research Institute Technical Report TCRL-24, 1983.

23. Tweedt, D. L. and Okiishi, T. H. Effects of Stator Blade Row Geometry Modification on Two-Stage Axial-Flow Compressor Aerodynamic Performance. Iowa State University Engineering Research Institute Technical Report TCRL-25, 1983.

24. Johnsen, I. A. and Bullock, R. O., Eds. Aerodynamic Design of Axial-Flow Compressors. NASA SP-36. 1965.

25. Smith, L. H., Jr. Wake Dispersion in Turbomachines. Journal of Engineering for Power, Trans. ASME 88: 688-690. 1966.

26. Propulsion and Energetics Panel Working Group 12. Through Flow Calculations in Axial Turbomachines. AGARD-AR-175. 1981.

27. Kluck, C. E. Prediction of Laminar-to-Turbulent Boundary Layer Transition in Axial-Flow Turbomachinery. Technical Report TCRL-21, Turbomachinery Components Research Program, Department of Mechanical Engineering and Engineering Research Institute, Iowa State University, Ames, Iowa, 1981.

28. Schäffler, A. Experimental and Analytical Investigation of the Effects of Reynolds Number and Blade Surface Roughness on Multistage Axial Flow Compressors. J. Eng. Power, Trans. ASME. 102: 5-13. 1980.

29. Schreiber, H. A. Untersuchung des geraden Verdichtergitters L030-4 bei schnallnahen Zuströmmachzahlen-Schaufelmittelschnitt des Transonikverdichterlaufrades 030. DFVLR IB 352-79/10. Oktober 1979.

30. Greitzer, Edward M. An Introduction to Unsteady Flows in Turbomachinery. Notes for ASME Short Course Program. Houston. March 1981.

31. Strazisar, A. J. and Hathaway, M. D. Unpublished correspondence and data from NASA Lewis Research Center research. 1982.

32. Weyer, H. B. Unpublished correspondence and data from DFVLR research. 1981.

END

FILMED

9-83

DTIC